BOTSWANA UNIVERSITY OF AGRICULTURE AND NATURAL RESOURCES

Department of Agricultural & Biosystems Engineering (ABE)

Assessing the potential of rainwater harvesting for sustaining small scale irrigated coffee farming in the Bigasha watershed, Uganda

by

Samuel Matyanga

Student ID: 202000796

Research thesis submitted to the Department of Agricultural and Biosystems Engineering in partial fulfilment of the requirement for the degree of Master of Science in Agricultural Engineering (Soil and Water Engineering stream)

Supervisors

1. Professor Rejoice Tsheko (Main supervisor)
2. Mrs Anne Clift-Hill
3. Professor Cecil Patrick

APPROVAL

.....	.....
Main Supervisor's Name and Signature	Date
.....	.....
Co-Supervisor's Name and Signature	Date
.....	.....
Co-Supervisor's Name and Signature	Date
.....	.....
Head of Department's Name and Signature	Date

DECLARATION

Except for those sections where references were provided to acknowledge the work from previous researchers, I, Samuel Matyanga, hereby declare that I am the first author of this dissertation and that this work has never been submitted either wholly or partially to any University or other institutions of higher learning known to me for any academic award.

Signature:

Date: 25/01/2023

ACKNOWLEDGEMENTS

With utmost sincerity, I begin by extending my heartfelt appreciation to the Almighty God for the matchless providence accorded to me throughout my two-year journey in Botswana for this Master's degree.

In the same vein, I extend my uttermost gratitude to my entire supervisory team that comprised of Professor Rejoice Tsheko as the main supervisor, Mrs Anne Clift-Hill and Professor Cecil Patrick as co-supervisors and Mr Jackson Ndiwa Aliwa and Dr Gilbert Gaboutloeloe as external advisers. It is for the meticulous support from this team, mentorship and tutorship, besides, the highly resourceful advice, counsel and guidance that enabled my successful completion of this research project.

In a special way, I wish to thank the officials from the Ministry of Water and Environment, the Uganda National Meteorological Authority and the Uganda National Agricultural Research Laboratories for the generosity and resourcefulness they exhibited while sharing the datasets that were used in this study. The list is long, but Dr Florence Grace Adongo, Dr Benon Zaake, Mrs Caroline Wafula, Mrs Vivian Nabyonga, Mrs Caroline Tumwebaze, Mr Maximo Twinomuhangi, Mr George William Omony, Mr Godfrey Mujuni, Mr Samuel Ekwacu, Dr Drake Mubiru and Mrs Jalia Namakula, your kind assistance is dearly appreciated.

Similarly, I wish to express my indebtedness to my sponsors the European Commission, for their commitment to fully fund this degree through the Mobility of African Scholars for Transformative Engineering Training (MASTET) scholarship.

Finally, it would be unjust if I do not recognise the selfless love, care, encouragement and support that Mr Kimera David and the family of Mr Jackson Ndiwa Aliwa have continued to provide to me in my academic endeavors. Your contributions are deeply appreciated and may the good Lord richly bless you.

DEDICATION

This research project is dedicated to my family members, relatives and friends, most notably: Mrs Susan Osire, Mr Mark Olweny Omalla, Mrs Robinah Olweny, Mr Martin Osinde, Mr Nicholas Opiri, Mrs Martha Olweny, Mr Asaph Olweny, Mrs Hildah Sarah Olweny, Mrs Juliet Osinde and my Cameroonian brother and confidant Mr Suh Neba Celestine, who stood with me through thick and thin to see to it that this two-year journey is a success.

ABSTRACT

This study used remote sensing, Geographical Information System (GIS), the Quantum GIS Soil and Water Assessment Tool (QSWAT+) and Crop Water and Irrigation Requirements Program (CROPWAT) to assess the potential of rainwater harvesting (RWH) for sustaining small scale irrigated coffee farming in the Bigasha watershed of Isingiro District in South-western Uganda. The study further demonstrated the benefits of geospatial analysis of large areas where non-spatially based methods have limitations by utilising the many capabilities and strengths found in the four tools selected above.

Despite the irrigation potential assessment studies conducted in the Bigasha watershed in recent years, which found the soils in this area to be suitable for coffee farming, production of the crop has been hampered by recurrent drought conditions (Droogers et al., 2012). Farmers were unable to implement irrigated coffee farming due to the lack of a reliable irrigation water source. Therefore, this study was carried out to assess the potential of RWH in the study area to supply the required irrigation water.

To identify potential RWH sites in the Bigasha watershed, four RWH site suitability analysis criteria were used: topography (slope), soils, land use and rainfall and runoff depth. Using ArcGIS 10.7 software, the raster maps for the slope and soil feature layers for the study area were created. The study made use of three temporal land use land cover (LULC) maps of 1999, 2010 and 2022. These maps were created by a supervised classification method using Landsat 7 (ETM+), Landsat 5 (TM) and Sentinel 2A (MSI) satellite imageries, acquired from the United States Geological Survey (USGS) and European Space Agency (ESA) databases.

The QSWAT+ software interface was used to integrate the input datasets of aforementioned criteria layers and further simulate the surface runoff from the Bigasha watershed. Subsequently, 62, 125 and 114 Hydrologic Response Units (HRUs), derived from the 1999, 2010 and 2022 LULC maps, respectively, were selected as potential RWH sites. The selected HRUs had the potential to generate an annual average surface runoff depth of at least 92 mm and require relatively small catchment area to harvest adequate amount of rainwater. The surface runoff volumes that could potentially be harvested from the three HRUs categories mentioned above were 1.61, 2.68 and 1.39 million cubic meters (MCMs), respectively.

Finally, the computed annual average gross irrigation water requirement of the coffee crop was 995 mm. This implies that the 1.39 MCM of rainwater in the Bigasha watershed that is currently potentially harvestable could irrigate up to 145 hectares (101.8 per cent) of small-scale coffee fields in the study area annually. The prediction accuracy of the Kagera river basin model was very good with NSE(R^2) values of 0.81(0.82) for calibration and 0.87(0.88) for validation. The Kagera watershed model fitted parameters were further used to calibrate the Bigasha watershed model. This was done because the Bigasha is a sub-basin of Kagera and does not have its own gauged outlet.

Key words*: Coffee farming; Irrigation; RWH; remote sensing; GIS; QSWAT+; CROPWAT; Bigasha watershed*

Table of Contents

List of Figures

List of Tables

List of Equations

List of Acronyms

ABE: Agricultural and Biosystems Engineering

CFSR: Climate Forecast System Reanalysis

CHIRPS: Climate Hazards Infrared Precipitation with Stations

CN: Curve Number

CROPWAT: Crop Water and Irrigation Requirements Program

DEM: Digital Elevation Model

DPU: District Planning Unit

DSMW: Digital Soil Map of the World

ESA: European Space Agency

ET_o: Reference Evapotranspiration

FAO: Food and Agricultural Organisation

GIS: Geographic Information System

HRU: Hydrologic Response Unit

ICO: International Coffee Organisation

ICRP: Irrigation for Climate Resilience Project

KNN: K-Nearest Neighbors

KRB: Kagera River Basin

LULC: Land Use Land Cover

MAAIF: Ministry of Agriculture, Animal Industries and Fisheries

MCM: Million Cubic Meters

MWE: Ministry of Water and Environment

NASA: National Aeronautics and Space Administration

NDP: National Development Plan

NRCS: Natural Resources Conservation Service

NSE: Nash Sutcliffe Efficiency

PBIAS: Per cent Bias

PPU: Per cent Prediction Uncertainty

QGIS: Quantum Geographic Information System

QSWAT: QGIS Soil and Water Assessment Tool

R^2: Coefficient of determination

RoU: Republic of Uganda

RWH: Rainwater Harvesting

SCS: Soil Conservation Service

SCP: Semi-automatic Classification Plugin

SUFI-2: Sequential Uncertainty Fitting

SPE: SWAT Parameter Estimator

SWAT: Soil and Water Assessment Tool

SWATCUP: SWAT Calibration and Uncertainty Program

UBOS: Uganda Bureau of Statistics

UCDA: Uganda Coffee Development Authority

UNMA: Uganda National Meteorological Authority

URWA: Uganda Rainwater Association

USDA: United States Department of Agriculture

USGS: United States Geological Survey

UTM: Universal Transverse Mercator

WGS: World Geodetic System

CHAPTER 1: INTRODUCTION

1.0 Background

Globally, Uganda is ranked as the eighth largest coffee producer, accounting for over 31 per cent of the total coffee exports from Africa, making it the second largest producer in Africa after Ethiopia (Miito & Banadda, 2017; UCDA, 2019b, 2019c; Nalunga, 2021). In 2019, Uganda's coffee sector was already employing an estimated five million people (ICO, 2019). Coffee accounts for over 20 per cent of Uganda's total foreign exchange earnings and 1.5 per cent of the annual gross domestic product (Jassogne et al., 2013; Akoyi & Maertens, 2018; UCDA, 2019b). During the coffee year 2021/2022, the country realised an export revenue of over US$ 741.03 million (UCDA, 2022).

The Uganda Coffee Development Authority noted that the global markets for both *Robusta* and *Arabica* coffee are sustainable and assured and that there is rising demand for good quality coffee. In 2020/2021, the global demand was 164.9 million bags which is projected to rise to 170.3 million bags by 2021/2022 (ICO, 2022). In 2021/2022, the global production is expected to be 167.2 million bags, 3.1 million bags less than the demand (ICO, 2022). According to UCDA (2019b) and Nalunga (2021), Uganda still has an immense untapped coffee production potential that if leveraged alongside good field husbandry and management practices such as irrigation could bridge the above coffee production gap and earn coffee farmers over Uganda shillings (UGX) 10 million per hectare per year.

During the year 2012, the Nile Basin Initiative irrigation potential assessment project identified suitable soils for coffee farming in the Bigasha watershed, located in South-western Uganda. These soils were categorised as ferralsols with an average land productivity of 0.6 based on the normalised difference vegetation index (NDVI), a figure that is higher than Uganda's average NDVI of 0.54 (Droogers et al., 2012). However, due to recurrent droughts in Bigasha, the area is characterised by low coffee production (MWE, 2019a; RoU, 2020c). The severity of drought is more felt in the months of December to February and June to August (Nyasimi et al., 2016). During these periods rainfall is low, yet evapotranspiration rates are high, exposing coffee plants to excessive moisture stress and resulting in a reduction in crop yield (FAO, 2015). For instance in 2017, drought contributed to nearly 60 per cent drop in coffee yield in Luwero district, one of the leading coffee growing districts in Uganda (MCDonnel, 2017).

The Food and Agricultural Organisation global information system on water resources and agricultural water management (FAO AQUASTAT) climatic statistics show that in the recent past (2010-2021), the annual average rainfall received in the joint sub-counties of Ngarama and Kashumba (where the Bigasha watershed is located) dropped to 960 mm. This is against a reference evapotranspiration rate of 1 347 mm, yet the coffee plant requires a minimum of 1 200 mm of water annually for its proper growth (UCDA, 2019b; AQUASAT, 2022). Nyasimi et al. (2016) noted that the current adverse variations in Uganda's climatic conditions would be exacerbated by increased frequency of occurrence and longevity of droughts, floods, etc., associated with global climate change. This was supported by MCDonnel (2017), who stressed that climate pressure could reduce potential coffee production by 50 per cent worldwide by 2050.

Therefore, adoption of irrigation by coffee farmers from the Bigasha watershed becomes paramount for successful coffee growing in this area. However, as pointed out by Droogers et al. (2012), the major impediment to irrigation practice in the Bigasha watershed is the lack of a reliable irrigation water source. There are two water sources adjacent to the watershed, namely, Lake Nakivale, which is located 20 kilometers away and would thus require substantial investments to convey water for irrigation and the Kagera river, which is a trans-boundary watercourse between Uganda, Tanzania, Burundi and Rwanda and hence requires formal approval from the Kagera Basin Organisation (KBO) to abstract water (Kagwanja, 2007).

Numerous efforts to address the water scarcity in the Bigasha watershed have been rendered by various development partners. This is evidenced by the construction of a total of 33 currently functional shallow wells, 32 deep boreholes, 1 019 rooftop rainwater harvesting tanks, 3 valley tanks, 3 protected springs and 61 piped water systems across the two sub-counties of Ngarama and Kashumba (MWE, 2019b, 2020a, 2022). However, most of these water sources are seasonal and are characterised by considerably low storage capacities. They often dry up at the onset of the dry season leaving only a few permanent sources that cannot even supply these sub-counties' two top priority demands which are domestic supply and livestock watering (RoU, 2020b). A case in point is Ngarama sub-county where only 48 per cent of the sub-county's 44 364 people have access to potable water throughout the year, a figure that is far below the national target of 66 per cent (MWE, 2019b, 2022). The question is, "How then shall irrigated coffee farming be fostered in the Bigasha watershed?".

In situ and/or ex situ rainwater harvesting (RWH), which is the collection and storage of local surface runoff, could potentially provide irrigation water for the small-scale coffee farmers in the Bigasha watershed. To harvest rainwater, a variety of locally known engineered and cost-effective techniques and structures could be used (Mugerwa, 2007; Stanley et al., 2020). The adoption of this prehistoric technology for agricultural production has become one of the indispensable adaptation strategies to the current adverse impacts of the global climate change (Kiggundu et al., 2018; RoU, 2020a).

Moreover, evidence of its successful application in coffee production has been found in many prominent coffee-producing countries, such as Brazil, Vietnam, Indonesia, Ethiopia, among others (Thao et al., 2019; Junqueira et al., 2020; Prijono & Sidauruk, 2020). Several benefits have been derived from rainwater harvesting for coffee farming among which include: protecting the coffee fields against soil erosion, providing water for irrigation and washing of pulped coffee, increasing soil moisture storage in coffee fields and above all improving the quality of coffee yields (Junqueira et al., 2020). For example, a study conducted by Adane & Bewket (2021) in Southern Ethiopia found that RWH can increase coffee yield by up to 70 per cent.

Similar findings have been reported from studies conducted in different coffee-growing regions of Uganda's neighboring countries, namely, Kenya, Tanzania and Rwanda (Wangui, 2012; Msuya, 2013; Hakorimana & Akcaoz, 2019). In Uganda, in-situ rainwater harvesting practices such as micro-pits, semi-circular bunds, Fanya juu bunds and soak away pits are the most commonly used for coffee farming (Kiggundu et al., 2018; Zziwa et al., 2018; Stanley et al., 2020). Studies conducted in five of Uganda's potential coffee growing districts, namely, Masaka, Rakai, Ibanda, Hoima and Kamwenge, found that RWH technology has the potential to sustain coffee production in the country (Kisekka et al., 2018; Zziwa et al., 2018; Stanley et al., 2020). A study conducted by Kisekka et al. (2018) in Ibanda, for instance, found that RWH can increase coffee yields by up to 66 per cent. Therefore, there is sufficient evidence of the feasibility of RWH for irrigation of coffee in water-stressed coffee-growing zones of Uganda, such as the Bigasha watershed.

1.1 Problem statement

Irrigation is recognised globally as the most appropriate technology for enhancing crop tolerance to the detrimental impacts of drought (MAAIF, 2017). Regrettably, irrigation adoption by small scale coffee farmers in the Bigasha watershed is still insignificant due to the lack of a reliable irrigation water source (Droogers et al., 2012). The approximated 960 mm of annual rainfall received in the Bigasha watershed could potentially be harvested to supply the required irrigation water (Nyirenda et al., 2021). Moreover, rain water harvesting may only supplement 20 per cent of the estimated 1 200 mm of water required annually to grow coffee in this area (UCDA, 2019b). However, there is limited information and knowledge about potential rainwater harvesting sites with maximum runoff yield not only in the Bigasha watershed but Uganda at large (RoU, 2020a).

Traditional non-spatially based methods for RWH site selection, such as surveying are indisputably the most accurate. However, these methods are time consuming and cost-ineffective, limiting their application to only small areas (Mosase et al., 2017). Yet, there is low adoption of the spatially-based RWH site suitability analysis methods across various agroecological zones of Uganda, possibly due to lack of knowledge of how to apply these methods, besides, scarcity of the input and validation data (Ammar et al., 2016; Kiggundu et al., 2018). Both multi-criteria analysis (MCA) and Artificial intelligence (AI) methods for RWH site selection are inapplicable in this study because they do not quantify the surface runoff from a watershed.

Therefore, the adoption of simple, flexible and above all accurate methods, such as geospatial techniques (remote sensing and GIS) integrated with hydrological models, specifically the QSWAT+ model, to assess the potential of RWH for sustaining small scale irrigated coffee farming in the Bigasha watershed becomes necessary. According to Ammar et al. (2016), remote sensing can be used to derive accurate information on thematic layers used for RWH site selection, with high spatial and temporal resolution, while GIS provides very useful tools for collecting, storing and analysing of both spatial and non-spatial data on the criteria layers. Similarly, hydrological modelling is a fundamental method for simulating surface runoff from any watershed, besides, providing a better understanding of the relationship between the upstream and downstream conditions of a watershed.

1.2 Significance of the study

Rainwater harvesting technology is reported to offer several contributions to agricultural production. These include: (i) reduction of crop moisture stress and improved yields, (ii) recharge of the ground water aquifers, (iii) mitigation of the effects of drought and improved resilience to drought, (iv) increased access to water by farmers and their livestock, (v) reduction in soil erosion due to minimal surface runoff and (vi) expansion of the total irrigated land. However, the above-mentioned benefits may not be realised if the RWH sites are not carefully selected. This study therefore provides resourceful knowledge and documentation about the effectiveness and reliability of the publicly accessible remote sensing, GIS and QSWAT+ model tools for rainwater harvesting site selection.

It is interesting to note that only a few, if any, and if not none of the previous studies conducted in Uganda have used geospatial techniques and hydrological models to select rainwater harvesting sites. On that note, the methodology adopted in this study has the potential to be replicated in other water-stressed agroecological zones of Uganda. The findings of this study provide a solid foundation for future implementation of RWH technology in the Bigasha watershed for policy makers, water managers, planners and farmers. This is because all the necessary information, such as the potential rainwater harvesting sites, the quantity of rainwater harvestable, coffee crop irrigation water requirements and the total area of the coffee field irrigable, is available.

The adoption of RWH technology is expected to improve coffee farmers' access to irrigation water during drought seasons in the Bigasha watershed. As a result, the adoption of irrigation by interested small scale coffee farmers may be accelerated. This would therefore ensure sustainable crop production and productivity in this area. Farmers' income may increase, livelihoods may improve and above all increased government revenue collections may be realised after the farmers sell their coffee produce. This is because coffee is so far the largest selling cash crop in Uganda.

1.3 Objectives of the study

1.3.1 Main Objective

The main objective of the study was to assess the potential of rainwater harvesting for sustaining small scale irrigated coffee farming in the Bigasha watershed, Uganda.

1.3.2 Specific Objectives

The main objective was met by the following specific objectives:

1) To characterise rainwater harvesting sites in the Bigasha watershed.
2) To map potential rainwater harvesting sites in the Bigasha watershed using remote sensing, GIS and the QSWAT+ model.
3) To determine quantities of harvestable rainwater at potential sites for irrigated coffee growing.
4) To estimate the total coffee production area that could be irrigated using this water.

1.4 Research Questions

The research questions that were answered at the end of this study for each of the objectives were:

Main objective

- ✓ Can rainwater harvesting sustain small scale irrigated coffee farming in the Bigasha watershed?

Specific Objective One

- ✓ What criteria was used for selecting potential sites for rainwater harvesting in the Bigasha watershed?

Specific Objective Two

- ✓ Which areas of the Bigasha watershed are best suited for rainwater harvesting and what is the total area of suitable sites?

Specific Objective Three

- ✓ What are the quantities of rainwater harvestable from the Bigasha watershed annually?

Specific Objective Four

- ✓ What is the irrigation water requirement for coffee grown in the Bigasha watershed?
- ✓ What is the total area where coffee can be irrigated with the harvestable rainwater at the Bigasha watershed?

1.5 Hypothesis

The validity of the hypothesis tested in this study was:

The Bigasha watershed has several potential sites for rainwater harvesting that if harnessed could provide enough water for small scale irrigated coffee farming. This could boost the production, productivity and profitability of coffee in the area.

CHAPTER 2: LITERATURE REVIEW

2.1 Coffee growing and its challenges in Uganda

Coffee is Uganda's primary cash crop contributing between 20 to 30 per cent of the country's annual export revenue and 1.5 per cent to the national GDP (Bunn et al., 2019; UCDA, 2019). The sector employs over 5 million people in Uganda (ICO, 2019). The majority (85 to 90 per cent) of Uganda's coffee farmers are small holder farmers whose average farm sizes are less than half a hectare. Only 10 per cent of the farmers own approximately one hectare of coffee farm plots (Bunn et al., 2019).

The coffee industry has registered a remarkable production growth from 2.03 million sixty kg bags, worth US$101 442 when the sector was liberalised in the year 1991/1992, to the current 6.72 million sixty kg bags worth US$ 741.03 million. This was primarily due to the expansion in the coffee cultivated area but the actual annual production fluctuates (Verter et al., 2015; Akoyi & Maertens, 2018; UCDA, 2022). For example, in the coffee year 1995/1996, the total coffee export quantity stood at 4.15 million sixty kg bags. This drastically dropped 10 years later to 2 million sixty kg bags. The export again rose to 3.58 million sixty kg bags in the year 2012/2013 before dropping to 3.31 million sixty kg bags in the year 2015/2016 (UCDA, 2006, 2013, 2017). The possible reason for the fluctuating production of coffee especially in the South-western parts of Uganda include: recurrent droughts, pest and disease outbreaks and aged coffee trees which are now less productive (Mukasa et al., 2020; UCDA, 2019c, 2022).

To maintain high coffee production, the adoption of irrigation is paramount in areas such as Bigasha if Uganda's coffee industry is to achieve its planned four-fold increase in production by 2025, as outlined in the Coffee 2025 Roadmap (Bunn et al., 2019). This is also stipulated in the Government of Uganda's third National Development Plan (NDP III) and Vision 2040 document (Bunn et al., 2019).

2.2 Irrigation development in Uganda: Constraints and Opportunities

Irrigation farming has been practiced in Uganda for over 120 years (Nakawuka et al., 2018). Unfortunately, to date, only 2.5 per cent of the country's 3.03 million hectares of irrigable land is irrigated despite the numerous crop losses that the country has continued to suffer due to recurrent droughts (Wanyama et al., 2017; Mukasa et al., 2020 Ssenyimba et al., 2020). In 2010, drought accounted for 38 and 36 per cent losses in Uganda's beans and maize production, respectively.

While in 2014, the country recorded 2.8 million normalised UGX (8 per cent) drop on its annual GDP (MAAIF, 2017).

With regards to coffee farming, the ICO (2019) report show that only 0.1 per cent of Uganda's 353 907 hectares of coffee fields are irrigated. Yet observations from irrigation farming in some parts of Uganda and beyond, show that irrigation is capable of mitigating droughts and increase crop yield by up to five times (MAAIF, 2017; Kimera et al., 2018). Generally, the assurance of receiving sufficient rains to sustain two cropping seasons under bimodal rainfall regimes has contributed to the low uptake of irrigation by Uganda's farmers (MAAIF, 2017). A major shift in the country's irrigation development was realised after the Uganda national irrigation policy was drafted in 2017, that set out priorities and strategies for irrigation development. This has so far seen the construction of about four medium scale and fifty small scale irrigation schemes across different parts of the country by various development partners (MAAIF, 2017; Sridharan et al., 2019; MWE, 2020).

From the technical point of view, Wanyama et al. (2017) identified inadequate access to water for irrigation, land tenure issues, economic aspects of irrigation and inadequate national irrigation capacity as the major hindrances to irrigation development in Uganda. Approximately 79 per cent of irrigated land in Uganda is under traditional irrigation especially around swampy areas (Ghanem et al., 2020). However, such systems could not be replicated in areas with no reliable water source which explains why the whole Isingiro district has no irrigation scheme, except the ongoing Kubuyanda irrigation scheme development project (MWE & MAAIF, 2020).

In this regard, the expansion of water for crop irrigation in water scarce areas such as Isingiro becomes essential if the Government of Uganda is to achieve its target of transforming the country's agriculture from subsistence to commercial agriculture through mechanization and irrigation (MAAIF, 2017; Bettili et al., 2019). This is equally emphasised in Uganda's national irrigation policy document, the NDP (II & III) and Vision 2040 (MAAIF, 2017). In the Uganda national irrigation policy, two strategic interventions specifically speak to the adoption of rainwater harvesting as a measure to augment water for production storage capacity in Uganda's agricultural sector (MAAIF, 2017). This is already incorporated in the ongoing irrigation for climate resilience project (ICRP), whose primary goal is to support the shift towards more resilient agriculture through the development of sustainable irrigation services (MWE & MAAIF, 2020).

2.3 RAINWATER HARVESTING (RWH)

Rainwater harvesting refers to a technology for collecting, concentrating and storing rainwater/runoff from rooftops, land surfaces or rock catchments using simple to engineered techniques for productive purposes such as crop, fodder, pasture and tree production, livestock watering, domestic water supply and ecosystems sustenance (Ibraimo & Munguambe, 2007; Mishra, 2014; Durodola et al., 2020). For agricultural applications, RWH is defined as a method of inducing, storing and conserving local surface runoff, mostly in arid and semi-arid regions (Hatibu & Mahoo, 1999; Ibraimo & Munguambe, 2007).

Approximately 50 – 70 per cent of the rainfalls received in the dry tropical regions across the world are lost as evaporation and/or surface runoff and hence inaccessible by crops (Rockström & Falkenmark, 2015). Consequently, 53 per cent increase in water supply to agricultural production becomes necessary if the targeted 70 per cent increase in the global food security by 2050 is to be achieved (Velasco-Muñoz et al., 2019). To reduce the aforementioned water losses, the adoption of strategic water resource management interventions such as rainwater harvesting becomes paramount in such dry tropical regions.

As reported by Ammar et al. (2016), RWH technology has been practiced worldwide for over 9 000 years. Although there is lack of quantification of the harvested rainwater used globally (Barron et al., 2009), RWH technology still forms an integral part of many farming systems by providing a reliable source of water. This is especially true for areas that receive significant amounts of rainfall but lack any conventional centralised supply system, owing to the temporal and spatial variability of rainfall (Ibraimo & Munguambe, 2007). For instance, studies conducted by Abdulla & Al-Shareef (2009) and Mourad & Berndtsson (2011) in the two arid countries of Jordan and Syria (with annual rainfall < 300 mm), found that approximately 15 and 35 MCM, respectively, of rainwater is harvested in these countries annually.

Similarly, Barron et al. (2009) reported that by adopting RWH technology, 15 million people in China had access to safe drinking water and 2.6 million ha of agricultural land was irrigated. Furthermore, Oweis & Hachum (2003) indicated that up to 50 per cent of rains received in the driest parts of West Asia and North Africa can be harvested with appropriate RWH techniques. In fact, increase in crop yields by up to 5 times have been realised from the adoption of RWH technology in many countries across the world, such as Tanzania, Kenya, India, among others

(Rockström & Falkenmark, 2015). In the Ugandan context, traditional practices such as use of banana stems as gutters and collection containers such as saucepans and pots, trenches and contour bunds etc., have been used since the 1950s (Kiggundu et al., 2018).

However, the formal introduction of RWH in the country started in 1997, with a primary target on institutional RWH (MWE, 2016; Zziwa et al., 2018). This later saw the formation of the Uganda Rainwater Association (URWA) in 1999, whose mandate was to "support communities to improve their socio-economic situation through mobilisation, information, skills and experience sharing" (URWA, 2013). Between 2003-2004, the Government of Uganda prepared a rainwater strategy aimed at promotion and building capacity of communities in RWH, primarily domestic rainwater harvesting (MWE, 2016). Since 2006, various development partners have been providing training and constructing numerous demonstration RWH facilities in different parts of Uganda (MWE, 2016).

2.3.1 Types of rainwater harvesting technologies in Uganda

There are two common types of RWH techniques in Uganda, namely, rooftop RWH and surface runoff harvesting, discussed in the following section.

2.3.1.1 Rooftop rainwater harvesting

Rooftop RWH is defined as a system of collecting rainfall from the roof of a building and storing it in storage facilities for domestic use, livestock watering or irrigation (Koskei, 2016; RoU, 2020b). The most common rooftop RWH storage facilities in Uganda include: saucepans, jerrycans, drums, ferro-cement tanks, rainwater jars, masonry tanks, Bob rainwater bag, among others (URWA, 2013). According to RoU (2020a), rooftop rainwater harvesting together with self-supply constitute 0.4 per cent of the rural water sources in Uganda. However, this technique's application in the country is limited to domestic water supply and to a limited extent agriculture because it is characterised by small catchment areas (rooftops) and low storage capacities as shown in Figure 2.1 (Kisakye et al., 2018; Koskei, 2016; RoU, 2020b).

The most common RWH technique in Isingiro district is rooftop RWH with over 3 538 functional rainwater storage tanks present in households, providing water to about 9 per cent of this district's population (MWE, 2020b, 2022). A similar trend is found in Ngarama and Kashumba sub-counties (where the Bigasha watershed is located) that together have a total of 1 019 rooftop RWH tanks alongside 3 earth dams and 3 valley tanks as shown by Table 2.1 below.

Table 2.1 Point water supply statistics for Ngarama and Kashumba sub-counties

Subcounty	Designation	Total population	Population served	Per cent access	POINT WATER SOURCES						
					Protected springs	Shallow wells	Deep boreholes	Rainwater harvesting tanks	Dams	Valley tanks	Stand pipes
Ngarama	Rural	44 364	21 279	48%	3	25	13	816	0	2	7
Kashumba	Rural	28 147	20 667	73%	0	8	15	203	3	1	54

(Source: MWE, 2022)

2.3.1.2 Surface runoff harvesting

Surface runoff harvesting refers to the collection, accumulation, treatment or purification and storing of storm water from a catchment for reuse in domestic supply, livestock watering and irrigation, among others (Chemutai, 2016; RoU, 2020a). It consists of a runoff generating area/catchment, transfer infrastructure such as channels, gullies and hard surfaces and a command area where runoff is utilised (Hatibu & Mahoo, 1999; Ammar et al., 2016; RoU, 2020a).

Surface runoff harvesting can be performed on micro or macro-catchments and studies across different parts of Uganda have reported the adoption of the technology (RoU, 2020b). Surface runoff harvesting techniques include: fanya-juu trenches, contour bunds, soak away pits, semi-circular bunds, ridges and mounds, terracing, trash-lines, road water harvesting, simple banana planting pits, farm ponds, valley tanks and earth dams (Kiggundu et al., 2018; Stanley et al., 2020). The last two (shown in Figure 2.1) are more common in the 121 cattle corridor districts in Uganda where they provide water for livestock (Maher et al., 2016).

Rooftop RWH

Valley tank

Earth dam

Figure 2.1 Rainwater harvesting techniques/systems in Uganda

2.4 Benefits of RWH and constraints towards its adoption in Uganda

Rainwater harvesting technology is not new to Ugandans and experiences of its practice across various parts of the country indicate that myriads of benefits can be realised from its use. Based on a study conducted by Kiggundu et al. (2018) in three of Uganda's cattle corridor districts, where RWH is extensively used for both livestock watering and irrigation of vegetables, coffee and tea seedlings, it was reported that RWH increased vegetable yields by up to five-fold which resulted in improved food self-sufficiency and house hold income. The same authors noted that RWH also reduced the burden to women, children and herdsmen of walking long distances in collecting and transporting water and hence they had adequate time to engage in other productive activities.

Similar results to those mentioned above were also reflected in the studies by Zziwa et al. (2018) and Stanley et al. (2020) who further noted that surface runoff harvesting contributed to reduction in soil erosion, moderation of floods, maintenance of soil nutrients, efficient use of pesticide and reduction in fertilizer loss. However, only 1 per cent of Uganda's 75 per cent rural farming population practice RWH despite the numerous benefits that it provides (MWE, 2016; Staddon et al., 2018; O'Hanlon et al., 2020). In other words, RWH technology contributes only 60 715 litres of water to Uganda's per capita annual water use of 6 071 571 litres (UBOS, 2021). This can be attributed to the limited knowledge of the potential of surface runoff harvesting across different agroecological zones in the country and appropriate techniques for RWH. Consequently, the RWH systems are either poorly sited or inappropriate technique(s) are chosen for particular areas (Kiggundu et al., 2018; Zziwa et al., 2018; O'Hanlon et al., 2020).

To address this challenge, MWE (2016) and Kiggundu et al. (2018) recommended the use of satellite products to: (i) map out potential runoff water harvesting areas in Uganda, (ii) estimate the potential yield from those catchments, (iii) establish the nature and level of pollutants contained in the harvested rainwater, (iv) assess the costs that are required to make the harvested water available for reuse as well as potential benefits and (v) evaluate profitability and risks associated with the use of this technology in different smallholder farmer setups. This research project sought to tackle the first two recommendations above, specifically in the Bigasha watershed.

2.5 Criteria and methods for determining potential sites for RWH

There are two approaches that are commonly used, namely:

a) ***Traditional non-spatially based method***

This involves conventional field surveys by specialists (soil, topography, land use etc.) of the area where the RWH project is to be implemented. Simple tools such as soil augers and levels may be used to identify sites with optimal biophysical characteristics for RWH (Ziadat et al., 2012; Mahmoud et al., 2015). Although this is indisputably the most accurate method for RWH site identification, it is time consuming and expensive and hence applicable to only small areas (Ammar et al., 2016; Mosase et al., 2017).

b) ***Spatially-based method***

Here, the parameters that determine the suitability of a site for RWH such as rainfall intensity and/or runoff depths, topography, land use land cover, soil texture/depth, etc., are analysed spatially (Oweis et al., 2012; Ammar et al., 2016). Firstly, using remotely acquired imagery (by satellites or other platforms), land use land cover, soil, grid interpolated rainfall (when using digital rainfall estimates) and other feature layers are derived at various spatial and temporal scales (Ganole, 2010; Munyao, 2010). Then with the help of the GIS spatial analyst tool, thematic maps for the feature layers are generated (Ammar et al., 2016).

Under the spatial-based analysis, several methods can be used to integrate these maps to identify possible RWH sites. These methods can be categorised into three groups, that is, multi-criteria analysis (MCA) techniques using either crisp or fuzzy sets, artificial intelligence (AI) methods and hydrological models (HMs). They can be applied either separately or within a GIS environment (Mahmoud et al., 2015; Mosase et al., 2017). The commonly used spatially-based RWH site suitability analysis methods are discussed in the following section.

2.5.1 Weighted linear combination (WLC)

This involves standardising each of the criteria maps, assigning weights of relative importance to each of them and generating a final RWH site suitability map of various suitability classes ranging from *most suitable* to *unsuitable* sites (Al-komaim et al., 2018; Toosi et al., 2020). The WLC is usually implemented in GIS using the raster calculator tool by a process known as weighted overlay process (Rana & Maruthi, 2020). One weakness of applying WLC alone is that criteria

weights are assigned based on the best compromise among competing interests (Ammar et al., 2016).

2.5.2 Boolean logic operators (AND/OR)

In this technique, the criteria maps for RWH site selection are reclassified into binary maps that are later merged/overlaid to generate a constraint map consisting of only two suitability classes that is, 0 for unsuitable areas and 1 for suitable areas (Bhowmick et al., 2014; Matomela et al., 2020). Although this method is simple and quick to implement, it is not flexible since it classifies RWH sites into strictly suitable and unsuitable sites (Aghaloo & Chiu, 2020; Matomela et al., 2020).

2.5.3 Analytic hierarchy process (AHP)

The analytic hierarchy process provides a structured technique for organising and analysing complex decisions in a hierarchical manner using mathematics and expert knowledge (Ammar et al., 2016). At the topmost level is the problem to be solved while the lowest levels contain details of factors influencing the problem (Ammar et al., 2016; Mulualem & Yegizaw, 2018). In AHP, two criteria are compared to each other in a pairwise comparison matrix consisting of a nine point scale of relative importance (Ammar et al., 2016; Al-Ghobari & Dewidar, 2021).

This comparison assists in assigning weights to the criteria after which normalised weights are generated using Eigen vector technique (Rana & Maruthi, 2020). The weighted criteria layers are then overlaid in GIS to generate a RWH suitability map (Ammar et al., 2016). Since AHP performs a consistency check on the judgments, it tends to reduce bias in decision making (Al-komaim et al., 2018).

2.5.4 Fuzzy logic/fuzzy sets

Here, the criteria layers are reclassified into fuzzy membership classes on a scale of 0 to 1 based on their contributions to RWH site selection (Manaouch et al., 2021). Zero (0) represents sites that are not members of the set while 1 represents sites that are certainly members of the set (Ajibade et al., 2020). Then using fuzzy overlay/fuzzy gamma operator in GIS, the fuzzified raster layers are integrated to generate a RWH suitability map (Aghaloo & Chiu, 2020; Chowdhury & Paul, 2021). The advantage(s) of the fuzzy logic MCA tool is that it models inexactitudes within class boundaries thereby reducing the ambiguity and imprecision of the decision maker in selecting cutoff points for the criteria layers (Mosase et al., 2017).

2.5.5 Artificial intelligence (AI)

The most applicable AI models in RWH site selection are the supervised learning classification and regression models such as random forest, support vector machines, neural networks, logistic regression and K-Nearest Neighbors (Al-Ruzouq et al., 2019; Meena et al., 2021).

Firstly, conditioning factors (thematic layers generated in GIS) for RWH site suitability analysis and a sample of point datasets are established (Al-Ruzouq et al., 2019) . The sample data is then divided into training and testing subsets usually in a ratio of seven to three. Each of these subsets of data alongside conditioning factors are then subjected to the AI algorithm to predict suitable RWH sites. Finally, the output of the AI model is digitised in GIS and a RWH site suitability map is generated (Naghibi et al., 2017). AI can be implemented using R-programming, python or other tools such as rapid miner. One of the most notable advantage of AI models is their high prediction accuracy (Rahmati et al., 2016; Naghibi et al., 2017).

2.5.6 Hydrological modelling (HM)

Hydrological modelling is the representation of the physical, chemical or biological characteristics of a catchment and simulating natural hydrological processes thereby facilitating the prediction of system behavior, understanding of various hydrological processes and decision making (Gayathri et al., 2015; Cloke & Schaake, 2020). It is commonly performed in areas where there is data scarcity, incomplete understanding, various alternatives to choose from and/or where experimentation with a prototype system is difficult (Cloke & Schaake, 2020).

With respect to RWH site suitability analysis, hydrological modelling is specifically used for estimating the amount of runoff that a particular catchment can generate. Here, point data for the feature layers such as land use land cover, soil, slope from digital elevation model (DEM) etc., are combined in a GIS environment to generate curve numbers (CNs), that are later processed as a grid to estimate runoff (Satheeshkumar et al., 2017).

Generally, evidence of the application of the spatially-based RWH site suitability analysis methods have been found in many countries around the world, especially those in arid and semi-arid regions such as India, Jordan, Syria, Iraq, South Africa, Tanzania, among others (Ammar et al., 2016). However, it is surprising that only a few, if any, of the above applications are from Uganda. This may be attributed to two factors: (1) lack of technical knowledge on the use of the spatially-based methods for RWH site selection, as highlighted by Kiggundu et al. (2018) and RoU (2020a) and

(2) scarcity of accurate input and validation data, which is common in developing countries (Ammar et al., 2016).

Therefore, the adoption of simple, flexible, accurate, time-efficient and cost-effective RWH site suitability analysis methods, such as hydrological modelling integrated with remote sensing and GIS, as reported by Ammar et al. (2016) becomes necessary not only in the Bigasha watershed but Uganda at large. This is because, as indicated earlier, HM is the only spatially-based method that quantifies the surface runoff that the watershed can generate during RWH site selection. Furthermore, the use of expert judgement when assigning weights of relative importance to the criteria layers in some MCA tools and AI models compromise the accuracy of these techniques for RWH site selection.

2.5.6.1 Classification of hydrological models

There are two broad classes of hydrological models, namely, deterministic models which give a single output for a set of inputs and stochastic models which give several outputs for a set of inputs (Gayathri et al., 2015; Cloke & Schaake, 2020). Rainfall-runoff models are deterministic models that can further be subdivided into six groups that is, empirical, conceptual, physically based, lumped, semi distributed and distributed models, depending on the physical principles applied in the model and temporal and spatial variability of the catchment parameters (Sitterson et al., 2017).

2.5.6.2 Review of commonly used rainfall-runoff simulation models

The application of models for hydrological studies has become indispensable in the recent years and with rapid advancements in computer technology, numerous computer-based hydrological/water quality general watershed models have been developed and applied globally to perform modelling tasks (Dhami & Pandey, 2013; Gayathri et al., 2015). The most common ones are: AnnAGNPS, GSSHA, VIC, Wet Spa, PRMS, SWAT, HYPE, WinSRM, DWSM, Hec-HMS, MODFLOW, HSPF and MIKE-SHE.

One of the most challenging tasks for potential model users is the choice of the best hydrological model for a particular application (Droogers et al., 2011; Dhami & Pandey, 2013). This is because these models vary substantially in the construction of their individual component processes that not only affects their modelling capabilities but also their overall accuracy (Gayathri et al., 2015). Therefore, it is crucial to make a thorough assessment of the model's capabilities and limitations before adopting it for any project.

Several researchers have compared various hydrological models in order to propose a more generalised hydrological model for global application (Dhami & Pandey, 2013; Sitterson et al., 2017). For example, Dhami & Pandey (2013) performed an intercomparison evaluation of nine commonly used, recently developed and regularly updated hydrological models viz: AnnAGNPS, GSSHA, WetSpa, PRMS, SWAT, HYPE, WinSRM, Hec-HMS and MIKE-SHE. This was based on the hydrological processes that the model can simulate, model's minimum input data requirements, governing equations used for simulating hydrological processes and the model's spatial scale. The results of this inter-comparison (Table 2.2) show that SWAT is the only continuous time scale, computationally efficient and publicly available model with manageable input data requirements and applicable to any size of watershed.

Table 2.2 Summary of common hydrological models and their application limitations

Hydrological model	**Modelling capabilities and limitations**
Hec-HMS (Hydrologic modelling system)	Cannot simulate all land phase processes of the hydrological cycle.
PRMS (Precipitation runoff modeling system)	Best suited for snow melt dominated watersheds and subject to computational instability if combined with other models.
MIKE-SHE (Système hydrologique européen)	Commercial model, extensive input data requirements and computationally unstable in case of large watersheds.
WetSpa (Water and energy transfer between soil, plants and atmosphere)	Applicable to a fixed watershed size (100 km^2 to 10 000 km^2).
GSSHA (Gridded surface subsurface hydrologic analysis)	Computationally intensive and subject to numerical instability in case of large catchments.
AnnAGNPS (Annualised agricultural non-point source)	Applicable to a fixed watershed size of 3 000 km^2 and cannot simulate ground water and snow melt.
HYPE (Hydrological predictions for the environment)	Best suited for continental and multi-basin simulations.
WinSRM (Windows snow melt runoff model)	Cannot simulate all land phase processes of the hydrological cycle, is a snow melt runoff simulation model and only simulates average daily discharge at the basin outlet.
SWAT (Soil and water assessment tool)	Has manageable input data requirements, is computationally efficient since it does not use numerical approximation-based equations, is applicable to any size of watershed and is publicly available.

(Source: Dhami & Pandey 2013)

2.6 Assessing the relevance of factors that determine technical suitability of a site for RWH

2.6.1 Slope

Slope of the catchment has been identified by most studies as one of the most important factors to consider when locating a RWH site, since it has a direct impact on the ease with which rainfall is transformed into runoff (Toosi et al., 2020). This is because the partitioning of rainwater between infiltration and runoff is greatly influenced by the topography of that given catchment (Toosi et al., 2020).

Landscapes with steep slopes are often considered least suitable for RWH because they are characterised by fast flowing runoff (reduced opportunity time) and hence demand large earthworks to create a RWH structure (Al-Ghobari & Dewidar, 2021). Furthermore, such slopes are prone to erosion and hence increased sediment loading problems occur (Adham et al., 2018; Khudhair et al., 2020). Ideally, catchments with fairly gentle slopes of less than 5 per cent constitute the best sites for RWH (Adham et al., 2018; Sayl et al., 2020; Toosi et al., 2020; Nyirenda et al., 2021).

2.6.2 Rainfall intensity and runoff depth

This is another influential factor for RWH site identification although most studies have not given it much attention (Ammar et al., 2016). In areas with a single rainy season, the annual average rainfall received in each watershed determines the cumulative amount of runoff that watershed can generate. Generally, it is expected that areas that receive high annual average rainfall are best suited for RWH and vice versa.

However, in the context of this study where there are two renown rainfall seasons, the first one running from March to May, also known as MAM and the second running from September to November, also known as SON (Onyutha et al., 2021), the average seasonal rainfall for each of these rainfall seasons and their corresponding surface runoff volumes could perhaps be considered instead. It is this surface runoff that could be used for irrigating the coffee crop in the intervening dry months June to August (JJA) and December to February (DJF).

For practical implementation of RWH systems, particularly ex-situ/macro catchment systems, a design rainfall of at least 200 mm/year is desirable (Toosi et al., 2020) while FAO recommends an annual rainfall range of 100 to 1 000 mm (Nyirenda et al., 2021). However, this should take into consideration other processes that occur during and/or after a rainfall event such as interception,

infiltration, evapotranspiration and deep percolation which have significant bearing on the percentage of rainfall that becomes runoff and this varies from catchment to catchment (Toosi et al., 2020).

2.6.3 Soil texture

Soil texture by definition refers to the proportion of sand, silt and clay particles which a soil contains (Rana et al., 2020; Al-Ghobari & Dewidar, 2021). It is another key criterion to consider when planning a RWH project. This is because just like slope, the texture of any given soil has a significant influence on not only the infiltration but also the runoff and water storage characteristics of that soil (Khudhair et al., 2020; Nyirenda et al., 2021).

Generally, naturally poorly drained fine to medium textured clayey soils have higher runoff generation potential and hence form more suitable sites for RWH compared to well drained coarse textured sandy soils (Naba, et al., 2018; Rasul et al., 2019; Shadmehri et al., 2020). The high water retention and runoff generation capacity of fine textured soils is attributed to the large number of micro pores within clay soils which restrict the movement of water down into the soil profile (Rana & Maruthi, 2020).

2.6.4 Land Use Land Cover (LULC)

Land use land cover equally plays a significant role in rendering a catchment suitable for RWH. The hydrological response of any watershed is dependent on land use land cover and the rainfall it receives and for many years hydrologists have found land use land cover patterns a notable factor to consider when evaluating the runoff dynamics of any watershed (Wu et al., 2018; Rasul et al., 2019).

Various land uses and vegetation covers have different impacts on the velocity and amount of runoff generated from a watershed (Rana et al., 2020; Toosi et al., 2020; Nyirenda et al., 2021). Dense vegetation and forest covered areas are often associated with high rainfall interception and water infiltration and hence are poor generators of runoff whereas built-up and pasture covered areas potentially generate high volumes of surface runoff (Adham et al., 2018; Al-Ghobari & Dewidar, 2021; Nyirenda et al., 2021).

2.7 SWAT model description

The soil and water assessment tool (SWAT) is defined as a continuous time, semi distributed, physically process-based and computationally efficient river basin model. It was first developed in the early 1990s for the United States Department of Agriculture (USDA), to evaluate the effects of alternative management decisions on water resources and non-point source pollution in large river basins (Zou et al., 2016; Diriba, 2021). The latest version is QSWAT+, which is a completely restructured version of SWAT with greater flexibility in representing the interactions and processes within a watershed (Bieger et al., 2017).

The model is capable of simulating a wide range of hydrological processes such as surface runoff, evapotranspiration, infiltration, percolation, shallow and deep aquifer flows, channel and reservoir routing (Efthimiou, 2018; Farzana et al., 2019). During simulations in SWAT, the watershed is first divided into multiple watersheds (subbasins), followed by landscape units (if necessary), which are further subdivided into hydrologic response units (Kaviya, 2013; Gayathri et al., 2015).

According to Dile et al. (2019), a subbasin is an area of land draining into a stream reach. Subbasins are the main subdivisions of a watershed whose SWAT outputs are generated and studied. They contain channels, which are finer divisions and extensions of stream reaches where the components of a watershed are precisely placed. These components are: landscape units, reservoirs, ponds, point sources and hydrologic response units (HRUs). Landscape units are areas draining into a channel reach and it is subdivided into the floodplain and upslope regions (Dile et al., 2022). The HRUs consist of homogenous land use, topographical, soil and management characteristics (Dile et al., 2022). However, Arnold et al. (2012) and Farzana et al. (2019) have indicated that the HRUs are represented as a percentage of the sub watershed area and may not be contiguous or spatially identified within SWAT simulation.

The two phases in SWAT simulation are the land phase, that controls the amount of water, sediment, nutrient and pesticide loading in the main channel of each subbasin, and the routing phase, that is concerned with the movement of water, sediment and agricultural chemicals through the channel network to the watershed outlet (Zou et al., 2016; Diriba, 2021).

The main propulsive force behind all land phase simulation processes in SWAT originates from the water balance equation expressed below (Kaviya, 2013; Ruan et al., 2017; Diriba, 2021):

$$SW_t = SW_o + \sum_{i=1}^{i} (P_{day} - Q_{surf} - E_a - W_{seep} - Q_{gw}) \quad \text{.....(2.1)}$$

where:

SW_t and SW_o are the final and initial moisture contents on day *i* (mm), *t* is time in days, P_{day} is the precipitation on day *i* measured in mm, Q_{surf} is the surface runoff measured in day *i,* E_a is the amount of evapotranspiration on day *i* (mm), W_{seep} is the amount of water that enters the vadose zone from the soil profile on day *i* (mm) and Q_{gw} is the return flow amount in day *i* (mm). The governing processes in SWAT modelling are surface runoff, evapotranspiration and channel routing as discussed below (Kaviya, 2013; Shanbor & Manoj, 2017).

a) Surface runoff

According to Kaviya (2013), Shanbor & Manoj (2017) and Diriba (2021), there are two methods used in SWAT for estimating surface runoff, namely, the Curve Number method developed by the USDA Soil Conservation Service (USDA SCS, 1972) and the Green and Ampt infiltration method (Green & Ampt, 1911). However, due to readily available daily rainfall data, most studies use the SCS-CN method whose general equation is given as:

$$Q_{surf} = \frac{(P_{day} - I_a)^2}{(P_{day} - I_a + S)} \quad \text{.....(2.2)}$$

where Q_{surf} is the accumulated runoff or rainfall excess (mm), P_{day} is the precipitation for the day (mm), I_a is the initial abstraction that includes surface storage, interception and infiltration prior to runoff and S is a retention parameter (mm) which varies spatially with the changes in the land features such as soil, land use, slope and management practices and temporally with soil water content (Kaviya, 2013). The S is expressed mathematically by the following equation:

$$(S = 25.4 * \frac{10}{CN} - 10 \quad \text{.....(2.3)}$$

The initial abstraction is usually approximated as 0.2S, whose substitution transforms equation 2.2 above to:

$$Q_{surf} = \frac{(P_{day} - 0.2S)^2}{(P_{day} - 0.8S)} \quad \text{.....(2.4)}$$

The value of the curve number is a function of land use practice, soil permeability and hydrologic soil group (Kaviya, 2013; Shanbor & Manoj, 2017). The selection of the hydrologic soil group(s)

used in the SWAT model is from the classification given by US Natural Resources Conservation Service (NRCS).

b) Reference evapotranspiration

SWAT provides three different options for estimating reference evapotranspiration that is: Penman-Monteith method (Monteith, 1965), Priestly-Taylor method (Prestley and Taylor, 1972) and Hargreaves method (Hargreaves et al., 1985) as cited by (Kaviya, 2013; Shanbor & Manoj, 2017 and Worku et al., 2017) . The choice of the method to use depends on data availability (Kaviya, 2013).

c) Channel routing

This belongs to the second phase of SWAT simulation processes and can be estimated using either the Muskingum method that models the storage volume in a channel length as a combination of wedge and prism storages or the variable storage method that uses a simple continuity equation in routing the storage volume (Shanbor & Manoj, 2017; Worku et al., 2017).

2.7.1 SWAT model sensitivity and uncertainty analysis, calibration and validation

According to Abbaspour et al. (2017), sensitivity analysis refers to the identification of the most important influence factor(s) in the model. Sensitivity analysis of model parameters is important because it provides information of the important processes in the study area and reduces the number of parameters in the calibration procedure by eliminating non-sensitive parameters (Abbaspour et al., 2017). The two common parameter sensitivity analysis performed in the SWAT model are the “one at a time” (local) and “all at a time” (global) sensitivity analysis (Abbaspour, 2021).

In the former, a single parameter is changed at a time to check its effect on the objective function, with the other parameters kept constant while in the latter, all parameters are changed at the same time (Abbaspour et al., 2017). The global sensitivity analysis method which produces the most reliable results uses the multiple regression approach to quantify the sensitivity of each parameter through the following expression (Abbaspour et al., 2017, 2021):

$$g = \propto + \sum_{i=1}^{n} \beta_i * b_i \quad \text{.....(2.5)}$$

where g is the value of the objective function, α is the regression constant, β is the coefficient of the parameters and b is the parameter. The above expression regresses the Latin hypercube parameters against the objective function values (Abbaspour, 2021).

Similarly, uncertainty analysis is the process of propagating all model input uncertainties to model outputs. These model input uncertainties may be caused by the modeler's lack of knowledge of the physical model inputs, namely, land use, soil and climate and/or the model parameters and structure (Abbaspour et al., 2017). Model calibration is the process of determining the best parameterisation of a model for a specified set of local situations thereby reducing the forecast uncertainty (Diriba, 2021).

During calibration, the parameter values are adjusted within the recommended ranges until the best simulation is attained (Arnold et al., 2012). Finally, model validation refers to the process of testing the calibrated parameter(s) with a new set of data. Validation of the model provides means for justifying that the developed model is capable of making satisfactory predictions (Refsgaard, 1997).

In the SWAT model, all the above tasks are performed with the help of the SWATCUP program (the current versions are: SWATCUP-2019, SWATCUP-Premium and SWATPlusCUP). The program has a graphical module for displaying simulation results, dotty plots to show the distribution of sampling points and visualise sensitivity of the parameters and the 95 per cent prediction uncertainty (95 PPU), *p* and *r* factors, for quantifying model uncertainties and goodness of the model (Abbaspour, 2021).

The common algorithms linked to the SWATCUP program that enables it to perform the calibration, validation, sensitivity and uncertainty analysis tasks are: the Generalised Likelihood Uncertainty Estimation, Parameter Solution, Particle Swarm Optimisation (PSO) and Sequential Uncertainty Fitting (SUFI-2). The latter was replaced by the SWAT Parameter Estimator (SPE) in the SWATCUP-Premium and SWATPlusCUP versions (Rouholahnejad et al., 2012). However, SUFI-2 and SPE are the most widely used algorithms. This is because they require fewer number of runs to reach acceptable calibration results (Amin & Nuru, 2020).

These algorithms map all uncertainties on the parameters and try to capture most of the measured data within the 95 per cent prediction uncertainty (95PPU) through an iterative process (Abbaspour

et al., 2015, 2021). The 95PPU is determined at 2.5 and 97.5 per cent levels of the cumulative distribution of an output obtained through Latin hypercube sampling (Abbaspour et al., 2015). The two commonly used indices to test the goodness of fit of the SWAT model when its outputs are expressed as uncertainty bands (95PPU band) are the *p* and *r*-factors (Amin & Nuru, 2020).

The p-factor is the percentage of the measured data bracketed by the 95PPU and it provides the measure of the model's ability to capture uncertainties (Amin & Nuru, 2020). On the contrary, the r-factor is a measure of the quality of the calibration and it indicates the thickness of the 95PPU, that is to say, the measured data that are not simulated well by the model (Amin & Nuru, 2020). Its value is computed by the following equation:

$$\mathrm{r-factor}\ \frac{\frac{1}{n}\sum_{ti}^{nj}(x_s{}^{ti,97.5\%} - x_s{}^{ti,2.5\%})}{\sigma_{obs}} \quad \text{.....(2.6)}$$

where $x_s{}^{ti,97.5\%}$ and $x_s{}^{ti,2.5\%}$ are the upper and lower boundary of the 95 PPU at a time step *t* and simulation *i*, n_j is the number of data points, and σ_{obs} is the standard deviation of the j^{th} observed variable. An ideal model should have a p-factor of 1 or 100 per cent and an r-factor of 0 or 0 per cent (Amin & Nuru, 2020). However, for stream flow, a p-factor of at least 0.7 and r factor of less than 1.5 is acceptable depending on the scale of the project and adequacy of the input and calibration data (Abbaspour et al., 2017).

2.7.2 SWAT model performance evaluation

The three widely used statistical indices (objective functions/efficiency criteria) for evaluating the performance of the SWAT model are: the coefficient of determination (R^2), Nash Sutcliffe efficiency (NSE) and per cent bias (PBIAS). The coefficient of determination is an indicator of the strength of the linear relationship between the observed and simulated data (Amin & Nuru, 2020). It measures how well the simulation versus the observation regression line approaches an ideal match. Its value is determined by the following equation:

$$R^2 = \frac{\sum_i^n(Q_{m,i} - Q'_m)(Q_{s,i} - Q'_s)^2}{\sum_i^n(Q_{s,i} - Q'_s)^2(Q_{s,i} - Q'_s)^2} \quad \text{.....(2.7)}$$

where R^2 is the coefficient of determination, $Q_{m.i}$ is the measured value of the i^{th} observed data, $Q_{s.i}$ is the simulated value of the i^{th} simulated output and Q'_m and Q'_s are the averages of the observed and simulated values, respectively (Abbaspour, 2021). The value of R^2 ranges from 0 to 1, where

0 indicates no correlation (Arnold et al., 2012). However, a value of at least 0.5 is satisfactory (Amin & Nuru, 2020).

The Nash Sutcliffe Efficiency indicates how well the plot of the observation versus the simulation fit on the 1:1 line (Amin & Nuru, 2020). The higher the value of NSE, the better the accuracy of the SWAT model and vice versa. A model with a negative NSE indicates very poor predictions and this implies that the average of the observed data is a better estimate than the model predictions (Arnold et al., 2012; Amin & Nuru, 2020). The value of NSE is determined by the following equation:

$$\mathrm{NSE} = 1 - \frac{\sum_i^n (Q_i - Q_s)^2}{\sum_i^n (Q_i - Q)^2} \quad \text{.....(2.8)}$$

where NSE is the Nash Sutcliffe efficiency, Q_i is the observed value, Q_s is the simulated value and Q is the average of the observed values (Abbaspour, 2021).

The value of NSE ranges from -∞ to 1 but a value of at least 0.5 is satisfactory (Amin & Nuru, 2020). Finally, the per cent bias measures the average tendency of the simulated data to be larger or smaller than the observations. A model with positive PBIAS is considered to be underestimating the phenomenon under investigation while that with a negative PBIAS is considered to be overestimating it (Gupta et al.,1999) as cited by (Abbaspour, 2021). Its value is determined using the following equation:

$$\mathrm{PBIAS} = 100 * \frac{\sum_i^n (Q_{m,i} - Q_{s,i})}{\sum_i^n Q_{m,i}} \quad \text{.....(2.9)}$$

where $Q_{m,i}$ and $Q_{s,i}$ are the observed and simulated values, respectively (Abbaspour, 2021). An ideal model should have a PBIAS of zero (0) per cent but a value ranging from ± 25 per cent is satisfactory (Amin & Nuru, 2020). A summary of the SWAT modelling processes is as shown in Figure 2.2 below.

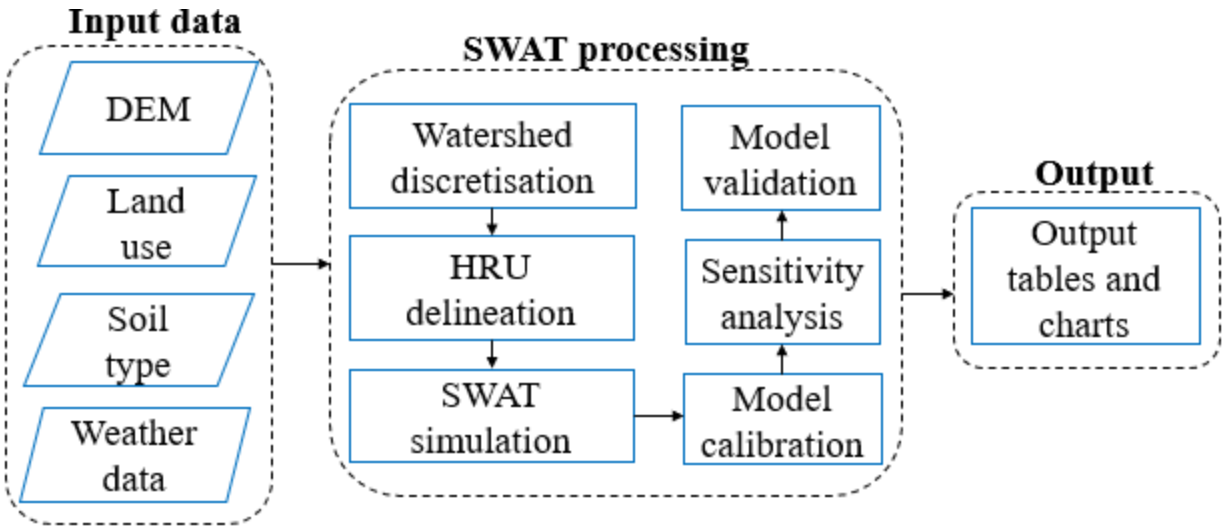

Figure 2.2 A typical SWAT modelling processes

(Source: Nilawar & Waikar, 2018)

2.7.3 Summary of the SWAT model runoff simulation results for RWH site selection

Over 4 000 publications in the SWAT database report on the application of various versions of the SWAT model for a range of purposes (Tan et al., 2020). For example, Janssen (2020) integrated the QSWAT model with the Google earth engine, python coding, Zoom earth and a socio hydrological model to estimate new reservoir locations for small holder cotton farmers in India. The findings of this study indicated that, of the existing 2 904 reservoir locations, only 2 474 qualified as potential locations thus indicating the need for the proper siting of new reservoirs in this area.

Similarly, Harka et al. (2020), Farooq et al. (2020) and Dwiatmojo et al. (2021) applied the ArcSWAT model for: identifying suitable RWH sites in Ethiopia, exploring surface runoff potential and RWH sites in Pakistan and mapping RWH potential in Indonesia, respectively. The results from the calibrated and validated model produced by Harka et al. (2020) show that ArcSWAT can satisfactorily predict stream flow (coefficient of determination (R^2) of 0.81 for calibration and 0.79 for validation and a Nash Sutcliffe efficiency (NSE) of 0.76 and 0.72, respectively). Neither Farooq et al. (2020) nor Dwiatmojo et al. (2021) calibrated their models but in Ethiopia, 553 potential RWH sites were found which together could generate a runoff volume of 154 million cubic meters while in Indonesia, there were 226 potential RWH sites with a runoff generating capacity of up to 494 969 m^3.

Other SWAT runoff simulation studies include: (i) runoff simulation in Tangnaihai hydrological station in the Yellow River in China by Li et al. (2020), whose results were R^2 and NSE of 0.77 and 0.76 during calibration and 0.90 and 0.89 for validation, (ii) rainfall runoff modelling study in ephemeral river basin in India by Bandi et al. (2020), with the results being R^2 and NSE of 0.83 and 0.85 during calibration and 0.83 and 0.67 during validation and (iii) hydrological modelling of Kangimi dam in Nigeria by Adeogun & Sanni (2019) where SWAT portrayed an excellent performance in the prediction of runoff inflow into the Kangimi dam with R^2 and NSE of 0.92 and 0.82 during calibration and 0.93 and 0.86 during validation.

2.8 CROPWAT model

The CROPWAT model is a Windows decision support system developed by FAO's Land and Water Development division in 1992, with the support of the Institute of Irrigation and Development Studies of the University of Southampton, United Kingdom and the National Research Center of Egypt. Its primary purposes are calculation of reference evapotranspiration (ET_o), crop water requirements (CWR) and irrigation water requirements (IWR) based on climatic and crop data (Dong, 2018; Aish et al., 2021).

However, it is also applicable in the development of irrigation schedules for different management conditions, calculation of scheme water requirement for various cropping patterns, evaluation of farmers' irrigation practices and estimation of crop performance under both rainfed and irrigated conditions (Feng et al., 2007; Stancalie et al., 2010; Laouisset & Dellal, 2016; Aish et al., 2021).

The latest version is CROPWAT 8.0 whose calculation procedures are based on two of the FAO publications in the Irrigation and Drainage series, namely, number 24 entitled 'Crop water requirements' and number 33 entitled 'Yield response to water' (Doorenbos et al., 1977, 1979).

The Penman-Monteith method is used by CROPWAT to compute reference evapotranspiration as per the recommendations of the expert consultative meeting organised by FAO in May 1990 in Rome (Smith, 1992; Allen et al, 1998; Moseki et al., 2019; Gabr, 2021) and its equation is expressed as:

$$ET_o = \frac{0.408\,\Delta((R_n - G) + 900\gamma)/(T_a + 273) * U_2\,(e_a - e_s)}{\Delta + \gamma(1 + 0.34U_2)} \quad \text{.....(2.10)}$$

where: ET_o is reference evapotranspiration (mm/day), R_n is net radiation at the crop surface (MJ/m^2/day), G is heat soil flux (MJ/m^2/day), T_a is average daily air temperature at 2 meters above

ground level (°C), U_2 is the wind speed at 2 meters above ground level (m/s), e_s is the saturation vapour pressure (kPa), e_a is the actual vapour pressure (kPa), Δ is the slope of the vapour pressure curve (kPa/°C) and γ is the psychometric constant (kPa/°C).

Penman-Monteith was recommended because it closely approximates grass evapotranspiration at the location evaluated, is physically based and explicitly incorporates both radiation (energy) and aerodynamic parameters (Allen et al., 1998). Moreover, procedures have been developed for estimating missing climatic parameters.

The crop water requirement, which refers to the amount of water lost by the field crop is computed in the CROPWAT model as a product of the crop coefficient (K_c) and the reference evapotranspiration as illustrated by the following equation:

$$ET_c = ET_o * K_c \quad \text{.....(2.11)}$$

where ET_c is the crop water requirement, ET_o is reference evapotranspiration and K_c is the crop coefficient, whose value varies with the crop's growing stage.

The net irrigation water requirement is computed as the difference between the crop water requirement and effective rainfall (Gabr, 2021; Alejo et al., 2021), as illustrated by the equation below:

$$IR_n = ET_c - P_e \quad \text{.....(2.12)}$$

where IR_n is the net irrigation water requirement, ET_c is the crop water requirement and P_e is the effective rainfall.

Depending on the irrigation system chosen, the gross irrigation requirement is computed as:

$$IR_g = IR_n / E_a \quad \text{.....(2.13)}$$

where IR_g(IR_n) are the gross(net) irrigation requirements and E_a is the irrigation efficiency obtained from local information or from the FAO 56 irrigation manual (Allen et al., 1998).

Therefore, in this research project, remote sensing, GIS and the QSWAT+ (latest version of SWAT) and CROPWAT 8.0 models were utilised to assess the potential of rainwater harvesting for sustaining small scale irrigated coffee farming in the Bigasha watershed.

CHAPTER 3: MATERIALS AND METHODS

This section discusses the steps that were undertaken to assess the potential of RWH for sustaining small scale irrigated coffee farming in the Bigasha watershed through the integration of remote sensing, GIS and the QSWAT+ and CROPWAT models, as summarised in Figure 3.2.

3.1 Description of the study area

3.1.1 Location

The Bigasha watershed is found in the Isingiro district, located in the absolute South-western part of Uganda. It lies between the latitude of 0º 48'30" S and 0º 59' 0" S and longitude of 30º 45' 30" E and 30º 59' 30" E as shown in Figure 3.1.

3.1.2 Topography

The Bigasha watershed's landscape can generally be described as undulating, with alternating highlands and lowlands spread throughout the watershed. The elevation ranges from 1 208 to 1 788 meters above sea level, based on the topography report generated by the QSWAT+ model in this work. Most slopes in the area are greater than 10 per cent and the watershed is drained by seasonal watercourses which flow into the Kagera river.

3.1.3 Land Use Land Cover

The watershed occupies a total land area of 34 793 hectares (~ 348 km^2). Croplands is the third largest land use type in the Bigasha watershed after grasslands and shrublands. The leading agricultural activities here are small scale banana growing and livestock rearing, with bananas accounting for nearly 70 per cent of the total annual crop production (DPU, 2015).

3.1.4 Soils

The predominant soil type in the Bigasha watershed are Leptosols. These are very shallow soils with minimal development, dominated by coarse fragments overlying a continuous rock mostly found in areas with medium to high altitude.

3.1.5 Climate and rainfall

The climate of the area is characterised as tropical savannah with annual average temperatures ranging from 15ºC to 27ºC. The annual average precipitation and reference evapotranspiration estimates are 954 mm and 1 347 mm, respectively (AQUASAT, 2022).

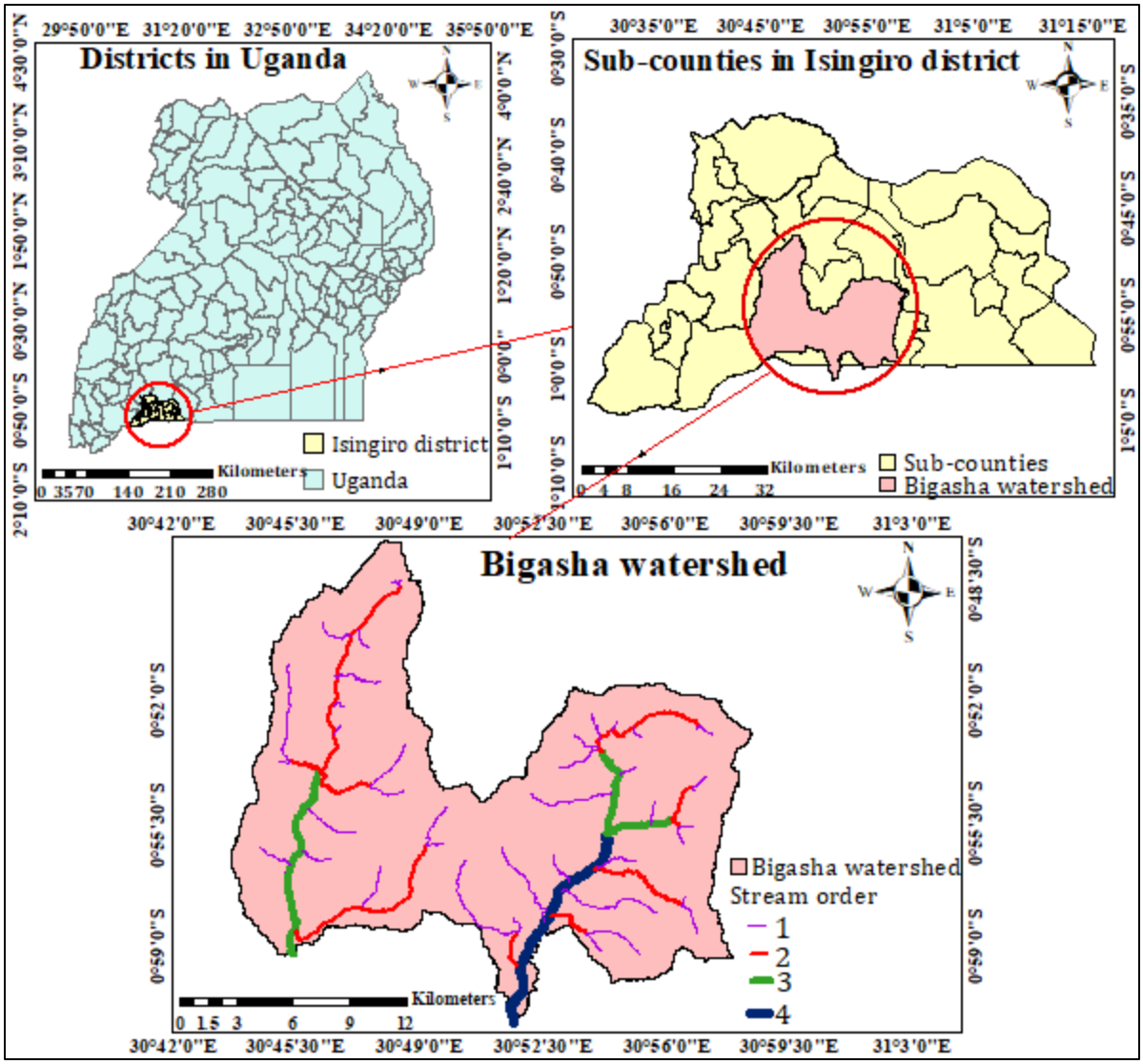

Figure 3.1 Map of the study Area

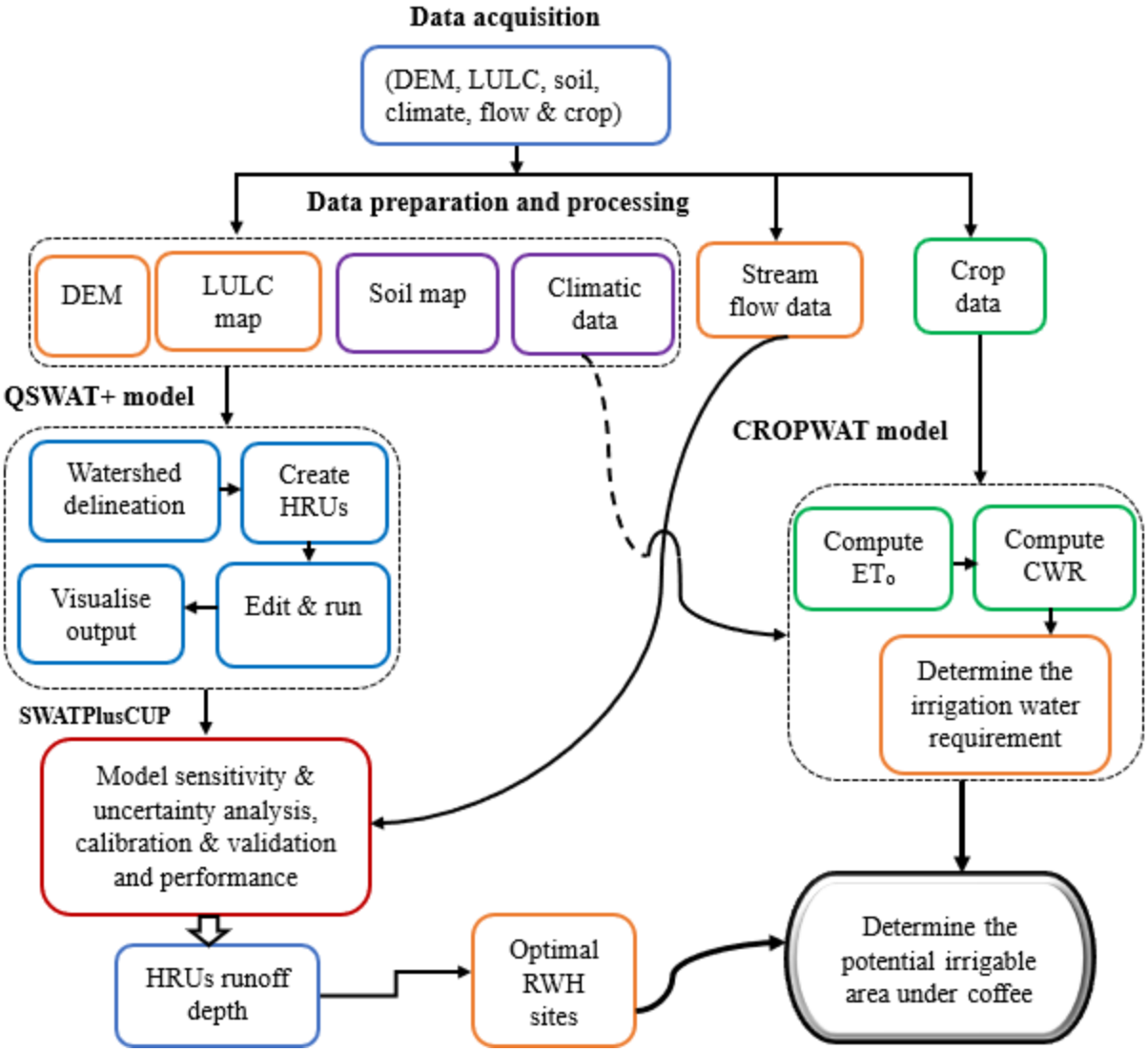

Figure 3.2 Steps in assessing the potential of RWH in the Bigasha watershed

3.2 Data sources

3.2.1 Digital Elevation Model (DEM)

A resampled 30-meter spatial resolution Shuttle Radar Topographic Mission (SRTM) DEM, which was part of the QSWAT+ model input data for watershed delineation was downloaded from the United States Geological Survey (USGS) database (www.earthexplorer.usgs.gov). This database was accessed through the 'SRTM Downloader' plugin installed in QGIS.

3.2.2 Land Use Land Cover (LULC) map

The LULC map was used for creating the HRUs in the QSWAT+ model. The three LULC maps used in this study were derived from three satellite images acquired between 1999 and 2022, with

a span of 11±1 years between their acquisition dates. These images were from the: Landsat 7 ETM+, Landsat 5 TM and Sentinel 2A sensors, acquired in 1999, 2010 and 2022, respectively. A Landsat TM image of 2010 was preferred over that of Landsat ETM+ acquired in the same year because the ETM+ images acquired in the 2000s were affected by the ETM+ scan line sensor error and hence difficult to classify without scan line error correction. It was for the same reason that the 1999 imagery was used in place of the 2000 imagery.

The Level 1TP ("precision and terrain correction") Landsat images were downloaded from the USGS database (www.earthexplorer.usgs.gov) while the Level 1C Sentinel imagery was obtained from the European Space Agency (ESA) data portal (www.copernicus.eu). Both the USGS and ESA data bases were accessed through the 'Semi-automatic Classification Plugin' (SCP) installed in QGIS. The downloaded image scenes were those with a cloud cover percentage of utmost 1 per cent. The acquisition dates (day and month) of the three images are not uniform (as shown in Table 3.1) because there were no image scenes with similar acquisition dates for all three of the images that had satisfactory cloud cover. The use of the three temporal LULC maps in this study was aimed at analysing the effect of land use change on runoff generation in the Bigasha watershed.

Table 3.1 Metadata for the LULC images

Image	Platform	Product Id	Acquisition date	Path	Row	Cloud cover	Spatial resolution	Scene center time
2022 Image	Sentinel-2A	S2A_OPER_MSI_L1C_DS_VGS4_20220112T091806_S20220112T081313_N03.01	12-01-2022	N/A	N/A	0.009	10 and 20 meters	08:13:11.024Z
2010 Image	Landsat-5 TM	LT05_L1TP_172061_20100815_20161014_01_T1	15-08-2010	WRS_PATH = 172	WRS_ROW = 061	1	30 meters	07:58:14.1280380Z
1999 Image	Landsat-7 ETM+	LE07_L1TP_172061_19990708_20170218_01_T1	08-07-1999	WRS_PATH = 172	WRS_ROW = 061	1	30 meters	08:00:40.8746889Z

3.2.3 Soil map

Like the LULC map, the soil map was also used to create HRUs in the QSWAT+ model. The soil map in "jpg format" was obtained from the Uganda National Agricultural Research Laboratories. The map had four soil types, namely, Orthic Ferralsols, Plinthic Ferralsols, Humic Gleysols and Leptosols (also known as Lithosols). The shapefile layer of the soil map was not available at the time of this study because the Uganda soils mapping database was being updated.

3.2.4 Meteorological data (2000 – 2020)

The climate data for simulating the runoff from the Bigasha watershed using the QSWAT+ model and calculating the irrigation water requirements of coffee in the CROPWAT model included: precipitation, relative humidity, wind speed, minimum temperature, maximum temperature, solar radiation and sunshine hours. The weather data for the first five variables were obtained from the records of the nearest meteorological station (Mbarara) from the Uganda National Meteorological Authority (UNMA) database.

The solar radiation data was obtained from the Climate Forecast System Reanalysis (CFSR) database, which was the recommended and most readily available global climate data source for the QSWAT+ model (Dile et al., 2022). The CFSR database has climatic data for five climate variables for a period between 1979 to July 2014. The sunshine hours data was not available and hence, the CROPWAT model sunshine hours estimates were used in this study.

3.2.5 Stream flow data (2001 – 2018)

This data was used for calibrating and validating the QSWAT+ model simulations. Since rivers within the Bigasha watershed are not gauged, the daily stream flow data from 2001 – 2018 recorded at the outlet of the Kagera river, whose contributing catchment, the Kagera river basin (KRB) covers the Bigasha watershed was used. This data was further processed to estimate the Bigasha watershed flow. The flow data was obtained from the Ministry of Water and Environment (MWE) in Uganda.

3.3 Data preparation and processing

3.3.1 Preparation of the QSWAT+ model input data

The input data required by the QSWAT+ model for simulating surface runoff were the DEM, LULC map, soil map, land use and soil lookup tables and daily climatic data (precipitation, minimum and maximum air temperature, wind speed, solar radiation and relative humidity).

3.3.1.1 Digital Elevation Model (DEM)

The resampled 30 m spatial resolution grids of the DEM downloaded from the USGS were loaded on the QGIS working space. Each loaded grid was clipped to extract a raster layer that covers the study area using the "Clip raster by extent" tool. The clipped grids were then merged with the help of the "Merge tool". The resultant grid of the DEM was reprojected to the Bigasha watershed's projected coordinate system (WGS 1984 UTM Zone 36S). The DEM was then resampled from 30 meters to 10 meters, to match with the spatial resolution obtained for the 2022 LULC image. Finally, to reduce time spent delineating the watershed as well as to improve accuracy, a rectangular mask of the DEM was created ensuring that it covered the entire study area as shown in Figure 3.3 below.

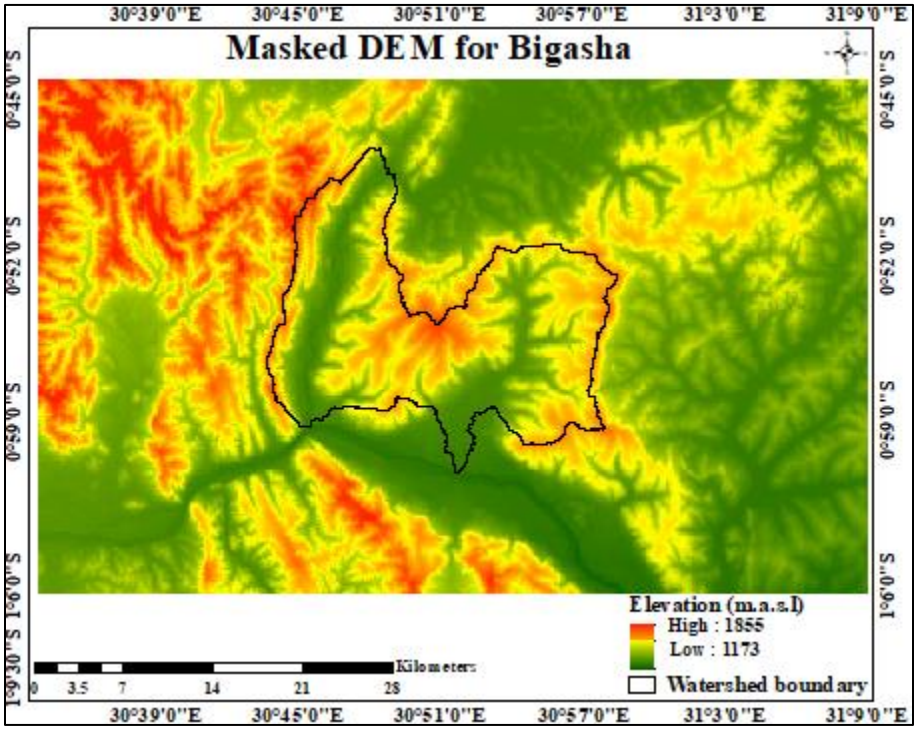

Figure 3.3 Masked DEM for the Bigasha watershed

3.3.1.2 Land Use Land Cover (LULC) map

The production of each of the three temporal LULC maps was performed in three stages, namely, image preprocessing, image classification and accuracy assessment. The procedures followed during image preprocessing and classification were those developed by Congedo (2021).

a) Image preprocessing

The downloaded image bands (Landsat or Sentinel bands, one product at a time) were loaded onto the semi-automatic classification plugin (SCP) interface, which was installed in QGIS. The SCP is a software interface that can be used for supervised classification of remote sensing images, providing tools for downloading the images and image preprocessing and post processing (Congedo, 2021). The image bands were then clipped to the extent of the study area using the "Clip multiple rasters" tool. The "dark object subtraction" atmospheric correction was then performed on the clipped image bands before they were converted to surface reflectance (Congedo, 2021).

b) Image classification

The images were classified using the SCP integrated with the KNN algorithm and Google Maps satellite image layer, all of which were installed in QGIS. The KNN classification algorithm is a non-parametric supervised machine learning algorithm, widely used for classification and regression tasks (Taunk et al., 2019; Yamaç, 2021). It was developed by Cover and Hart (1967), as cited in (Yamaç, 2021), for executing characteristic analysis where clear parametric approximations of probability densities are either unknown or difficult to determine. There are two steps in the classification process of the KNN algorithm, that is to say, the learning and the evaluation steps.

In the learning step, the training input data is used to build the classifier. This step involves determining the factor of K, which is a parameter that determines the number of nearest neighbors to include in the majority voting process. While the evaluation step involves assessing the prediction accuracy of the classifier, based on the values of the "classification precision" obtained from the confusion matrix of the classification accuracy assessment report. Once the factor of K is known, the KNN algorithm groups the new input unclassified data into subsets and classifies it based on its similarity with previously trained data (Taunk et al., 2019). Taunk et al. (2019) further noted that the KNN algorithm can divide the input datasets into different classes in a much clearer way which increases its prediction accuracy.

The image classification was performed as follows: firstly, the “band set” for the preprocessed image bands was created within the SCP interface and its color composite (red, green, blue) also known as RGB was changed for easy visual interpretation of the land use land cover features. The training input shapefile was then created inside the “SCP dock” window of the SCP. The SCP dock is an interface in the SCP menu that allows for the creation of regions of interest (ROIs) and spectral signatures required for the classification of a band set (Congedo, 2021).

The regions of interest (ROIs) were created hereafter through an iterative process. The creation of each ROI involved drawing of a polygon, covering pixels of the same spectral signature on the image being classified. Each ROI corresponded to a LULC Class ID (C ID). The created C IDs were then grouped into eight macro class IDs (MC IDs) which represent the eight LULC classes in the Bigasha watershed. The identified LULC classes were forests/trees, shrublands, grasslands, croplands, built-up areas, water bodies, bare land and flooded vegetation.

The Google satellite map and the “Display NDVI” option in the SCP dock were used to assign the correct LULC classes to the ROIs created. Finally, the KNN algorithm was run to execute the classification task. It is important to note that the final classified image was obtained after several classification runs in the KNN classifier to improve the accuracy of the classification. KNN classifier was chosen for its simplicity, effectiveness (high prediction accuracy) and low computational time (Taunk et al., 2019), compared to other classifiers. The classification stages discussed above are summarised by the workflow shown in Figure 3.4 below.

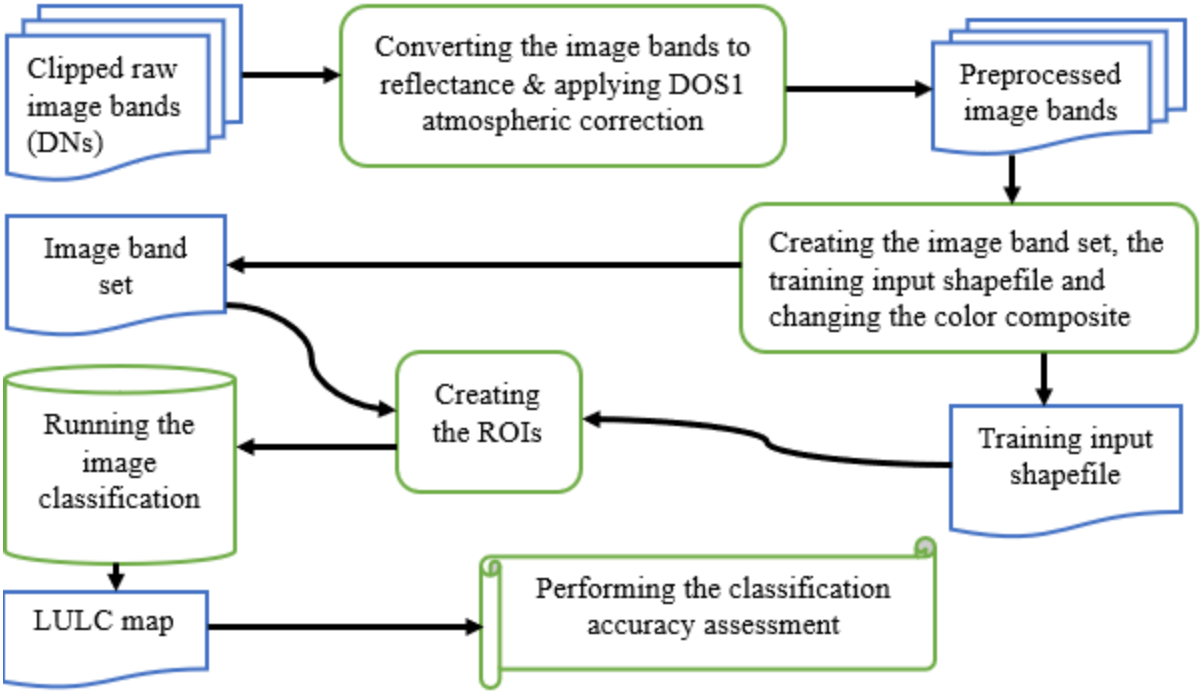

Figure 3.4 LULC map classification workflow

c) Accuracy assessment

According to Plourde & Congalton (2003), it is important for a user to know the accuracy of a classified LULC image in order to use it more correctly and efficiently. The accuracy assessment for each of the three LULCs was performed using the error matrix method. This is the most widely used method for assessing the accuracy of a LULC classification process (Strahler et al., 2006; Rwanga & Ndambuki, 2017). This is because the procedures involved in the derivation of the error matrix and the subsequent calculations produce four indices which represent the classification accuracy (Congalton, 1991) as cited by Manandhar et al. (2009).

These indices are the user, producer and overall accuracies and Kappa coefficients. To perform the accuracy assessment, a point feature shapefile with “Ground truth” and “Reference” fields in its attributes table was first created in QGIS. The classified LULC image was then loaded onto the same QGIS map canvas having the point shapefile. A stratified random sampling scheme, as recommended by Congalton (1991), was then used to collect sample points from each of the eight LULC feature classes on the classified image. This sampling technique minimises possibilities of under sampling that are often witnessed with simple random sampling method (Congalton, 1991). For example, the sampled points on the 2022 LULC classified image is shown in Figure 3.5 below.

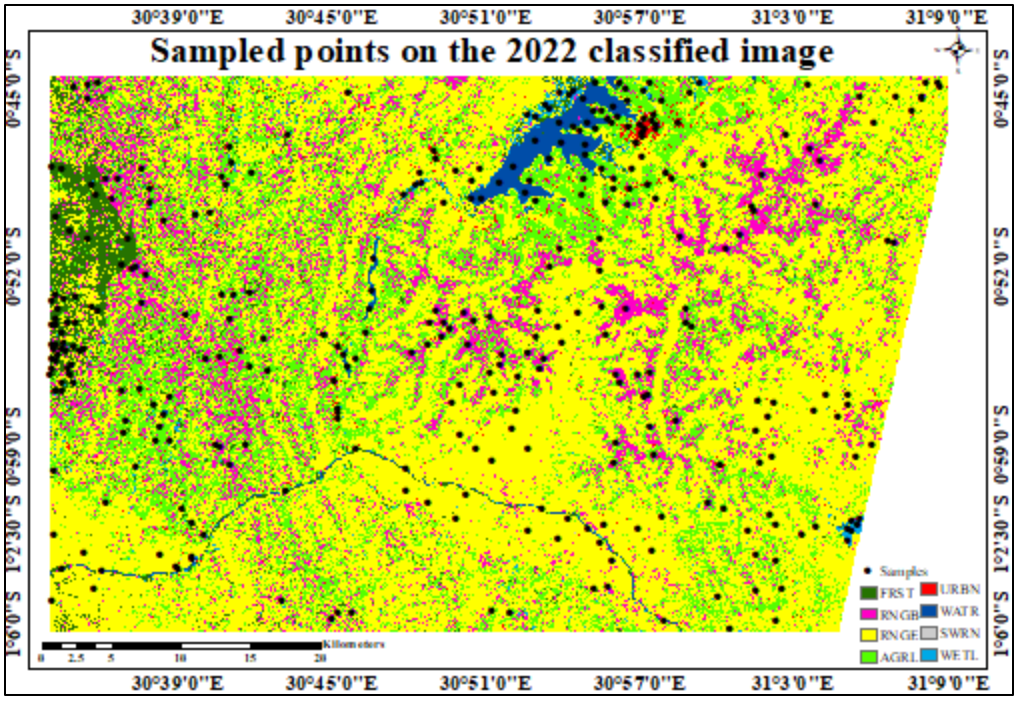

Figure 3.5 Sampled points used for accuracy assessment on the 2022 LULC image

After gathering at least 270 sample points from the eight LULC classes, the shapefile was uploaded onto Google Earth Pro and its "Reference" field was filled with the actual land cover IDs. Using the "show historical imagery" option in Google Earth Pro, an imagery with a close acquisition date to that of the LULC image being validated was selected. This was done to minimise the differences in the temporal resolution of the classified and reference images.

The sample size collected from each LULC category depended on the inherent spatial variability of the LULC category, as recommended by Congalton (1991). In other words, the larger the area of the LULC class, the higher the number of sample points that were collected on it and vice versa. The filled point shapefile was then imported to ArcGIS 10.7 software to generate the error matrix shown in Table 3.2, in the case of the 2010 LULC image. This error matrix was later copied and pasted on an Excel sheet and the user, producer and overall accuracies and the Kappa coefficients were calculated using the following expressions:

$$\text{User accuracy} = \frac{\text{Number of correctly classified pixels in each category}}{\text{Total number of pixels in that category (row total)}} * 100 \quad \text{.....(3.1)}$$

$$\text{Producer accuracy} = \frac{\text{Number of correctly classified pixels in each category}}{\text{Total number of pixels in that category (column total)}} * 100 \quad \text{.....(3.2)}$$

$$\text{Overall accuracy} = \frac{\text{Total number of classified pixels (diagonal)}}{\text{Total number of reference pixels}} * 100 \quad \text{.....(3.3)}$$

$$\text{Kappa coefficient} = \frac{(\text{TS} * \text{TCS}) - \sum(\text{column total} * \text{row total})}{\text{TS}^2 - \sum(\text{colum total} * \text{row total})} \quad \text{.....(3.4)}$$

where TS represents the total number of sample points and TCS is the total number of correctly classified pixels.

In case the computed overall accuracy was less than the minimum acceptable accuracy of 85 per cent proposed by Anderson et al. (1976) as cited by Manandhar et al. (2009), the image was reclassified. Finally, the 1999 and 2010 LULC classified images from the Landsat were resampled from 30 m to 10 m, to match with the spatial resolution obtained for the 2022 classified image.

Table 3.2 Error matrix for assessing the accuracy of the classified image of 2010

Reference Value	Ground truth 1	Ground truth 2	Ground truth 3	Ground truth 4	Ground truth 5	Ground truth 6	Ground truth 7	Ground truth 8	User sum	User accuracy
1	**27**	0	0	0	0	0	0	0	27	100.0
2	0	**45**	2	4	0	0	0	0	51	88.2
3	0	0	**62**	2	0	0	0	0	64	96.9
4	0	0	0	**39**	0	0	0	0	39	100.0
5	0	0	0	0	**10**	0	0	0	10	100.0
6	0	0	0	0	0	**30**	0	0	30	100.0
7	0	0	0	0	1	0	**17**	0	18	94.4
8	0	0	0	0	0	0	0	**33**	33	100.0
Producer sum	27	45	64	45	11	30	17	33	**272**	**97.4**
Producer Accuracy	100.0	100.0	96.9	86.7	90.9	100.0	100.0	100.0	**96.8**	**263**

NB: Total number of classified pixels (TCS) was 263, total number of reference pixels (TS) was 272, product of the total number of reference pixels and total number of classified pixel (TS *TCS) was 71 536, summation of the product of the column total and row total was 11 280 and finally, the square of the total number of reference pixels was 73 984.

3.3.1.3 Soil map

The soil map for the Bigasha watershed was created with the help of ArcGIS 10.7 software. Firstly, the acquired soil map was loaded onto ArcGIS and it was georeferenced using the administrative boundaries shapefile layer for Isingiro district. It was reprojected to the Bigasha watershed's projected coordinate system (WGS 1984 UTM Zone 36S). The resultant map was converted to a raster and later to a polygon using the "raster to polygon" spatial analyst tool in ArcGIS. The map

was then resampled to 10 m, to match with the spatial resolution obtained for the 2022 LULC image.

The World Reference Base (WRB) soil names in the attributes table of the soil map were then converted to the FAO soil symbols that is recognised by the QSWAT+ model. The FAO soil symbols that were assigned to the four soil types of the processed soil map were Fo43-2b, Fp10-2a, Gh7-2a and I-U-c, representing Orthic Ferralsols, Plinthic Ferralsols, Humic Gleysols and Leptosols, respectively. The symbol for Lithosols was used to represent Leptosols because Lithosols are equivalent to Leptosols in the FAO soil taxonomy (Gliński et al., 2008).

3.3.1.4 Land use land cover and Soil lookup tables

The LULC and soil map look up tables were used for linking the land use and soil maps to the QSWAT+ model and they were both prepared as comma separated (csv) files. The LULC lookup table had a land use text string in its file name and its structure was similar to that of the global land uses table in the QSWATPlusProj@2018.sqlite database. This is the recommended land use lookup table file structure for the QSWAT+ model (Dile et al., 2022). The lookup table had two columns, the land use identifier (LANDUSE_ID) and the SWAT_CODE. The SWAT_CODEs assigned to the eight LULC classes in the Bigasha watershed were FRST, RNGB, RNGE, AGRL, URBN, WATR, SWRN and WETL for forests/trees, shrublands, grasslands, croplands, built-up areas, water bodies, bare land and flooded vegetation, respectively, as shown in Table 3.3 below.

Table 3.3 The land use lookup table

LANDUSE_ID	SWAT_CODE
1	FRST
2	RNGB
3	RNGE
4	AGRL
5	URBN
6	WATR
7	SWRN
8	WETL

Similarly, the soil lookup table had the soil text string in its file name and its structure was similar to that of the global soils table in the QSWATPlusProj@2018.sqlite database. This is the

recommended soil lookup table file structure for the QSWAT+ model (Dile et al., 2022). The lookup table had two columns, the soil identifier (SOIL_ID) and the soil name (SNAM) columns. The SNAMs assigned to the four soil types in the Bigasha watershed soils were Fo43-2b-498, Fp10-2a-560, Gh7-2a-57 and I-U-c-3132 for Orthic Ferralsols, Plinthic Ferralsols, Humic Gleysols and Leptosols, respectively, as shown in Table 3.4. The "global user soil" file was used to assign soil properties to the soils.

Table 3.4 The soil lookup table

SOIL_ID	SNAM
57	Gh7-2a-57
498	Fo43-2b-498
560	Fp10-2a-560
3132	I-U-c-3132

3.3.1.5 Daily observed weather data

The station information for all the five climatic variables (precipitation, solar radiation, wind speed, relative humidity and maximum and minimum temperature) were first prepared in *.txt files. Each station file contained the station Id (ID), station name (NAME), latitude (LAT), longitude (LONG) and the altitude (ELEVATION). For example, the precipitation station *.txt file is as shown in Figure 3.6 below.

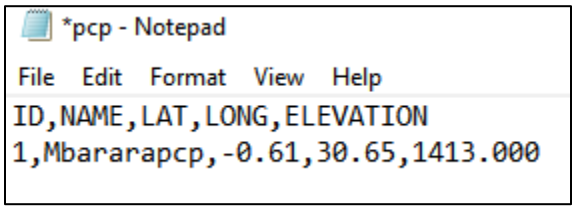

Figure 3.6 Precipitation station information for the Bigasha watershed

The observed weather data (*.txt) files for the climatic variables were then prepared. The information included in the observed weather files were the starting date of the measurements and the actual measurements. The starting date, 01/01/2000, was written in the first line of the observed weather files while the actual weather measurements were written in the succeeding lines, as required by the QSWAT+ model. The format in which the daily measurements for precipitation, solar radiation, wind speed and relative humidity were written in their respective *.txt files was

the same, as shown partially in Figure 3.7, in the case of the precipitation data. The maximum and minimum temperatures, however, were both written in one *.txt file but with their daily measurements separated by commas, as shown partially in Figure 3.7, as required by the QSWAT+ model.

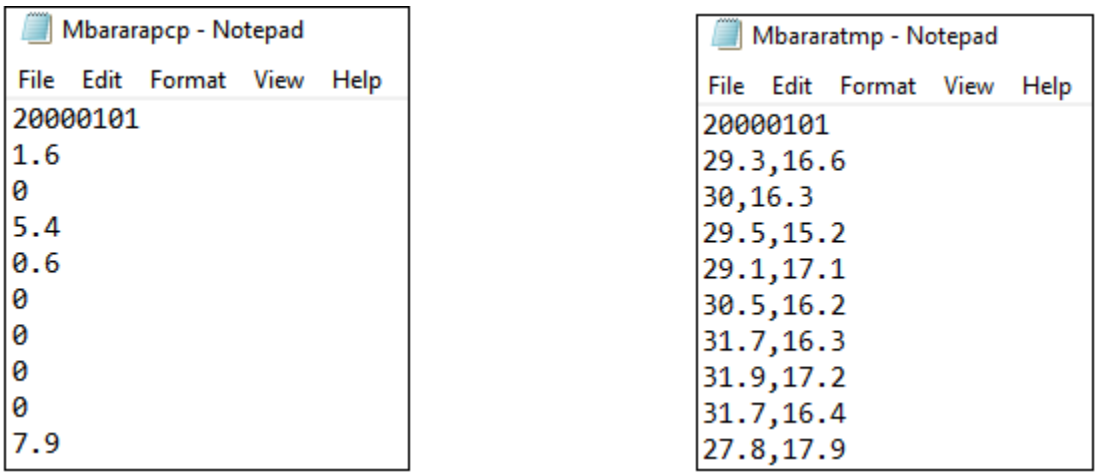

Figure 3.7 Samples of precipitation (left) and temperature (right) text data files

It is important to note that except for air temperature, the data for the remaining climatic variables had gaps. The missing climate data for the days between 1/1/2000 and 31/7/2014 were filled with CFSR data while those after July 2014 were filled with -99 (Dile et al., 2022). The periods with missing data are shown in Table 3.5 below.

Table 3.5 Periods with missing observed weather data

Climate variable	**Periods with missing data**			
Rainfall	May 2004	April 2005	October 2006	April 2009
Solar radiation	2000 – 2020			
Wind speed	2000 – 2004		2016 – 2020	
Relative humidity	2000 – 2004		2020	

3.3.1.6 Observed stream flow data

The monthly stream flow records for the Kagera river covering a period of 18 years (2001 – 2018) were prepared in a Microsoft Excel file. This file had two columns with the same number of rows.

The first column had the “Date” when the data was acquired (year and month, written as: YYYY/MM) while the second had the monthly “Flow” data itself, as shown partially in Table 3.6. The months with missing observed flow data, for example from January 2001 to March 2001 and from August 2005 to April 2006, were included in the Excel file since dates are sequential. However, their corresponding stream flow data cells were left blank (Dile et al., 2022).

Table 3.6 Sample of the monthly stream flow data for the Kagera river

Year/month	Flow (m^3/s)
2001/4	151.75
2001/5	111.14
2001/6	107.06
2001/7	104.45
2001/8	99.01
2001/9	95.31
2001/10	97.76
2001/11	111.52
2001/12	101.73

3.3.2 Preparation of the CROPWAT 8.0 model input data

The input data sets required for calculating the irrigation water requirement of the coffee crop in the CROPWAT 8.0 model were climatic data (precipitation, relative humidity, minimum temperature, maximum temperature, wind speed and sunshine hours) and crop data (Dong, 2018; Aish et al., 2021). The monthly weather data of the first five climatic variables listed above, for periods with available data were compiled using Microsoft Excel. The monthly precipitation was obtained by summing the daily rainfall measurements while the monthly values for relative humidity, air temperature and wind speed were obtained by averaging daily measurements. For the months where the climate data was missing, CFSR data was used to fill the gaps for periods between 2000 and July 2014 while CROPWAT model estimates were used to fill those for periods after July 2014.

An attempt was made to estimate the mean relative humidity (RH) using the procedures described in the FAO 56 manual, for areas with tropical climates. This was done because the RH data set obtained from the UNMA is usually recorded at 9 am (to represent maximum RH) and 3 pm (to represent minimum RH) East African time and hence may not represent the actual peak and minimum humidity conditions in the watershed. However, this did not yield meaningful results

since the estimated RH values were lower than the measured ones. Therefore, the observed RH data from UNMA was used.

The coffee crop information required in the CROPWAT model was the length of crop growing stages, the crop coefficient (K_c), the critical depletion factor (p), the rooting depth (Z) and the yield response factor (K_y). These were obtained from the Uganda coffee handbook and FAO Irrigation and Drainage papers 33 and 56 (Doorenbos et al., 1979; Allen et al., 1998; UCDA, 2019). The value of K_y used in this study was that for citrus since there was no value of K_y given for coffee. Afterall, the length of crop growing stages, crop coefficients (K_c) and annual irrigation requirements of coffee and of citrus are not significantly different (Doorenbos et al., 1979; Allen et al., 1998; Tobergte & Curtis, 2013).

3.4 Data analysis

3.4.1 Building of the QSWAT+ model for the Bigasha watershed

The model was built within the software interfaces of QGIS (version 3.2.29), QSWAT+ (version 2.2.5) and the SWAT+ Editor (version 2.1.3), using the procedures developed by Dile et al.(2022). The tasks undertaken here were the creation of the new QSWAT+ project, watershed delineation, creation of the HRUs, importation of the weather data and running of the QSWAT+ model and visualising of the model outputs, respectively. These were performed as follows: firstly, the QGIS software was started and the QSWAT+ plugin was opened. The new QSWAT+ project named "Bigsam" was then created in the QSWAT+ model interface, as shown in Figure 3.8 below.

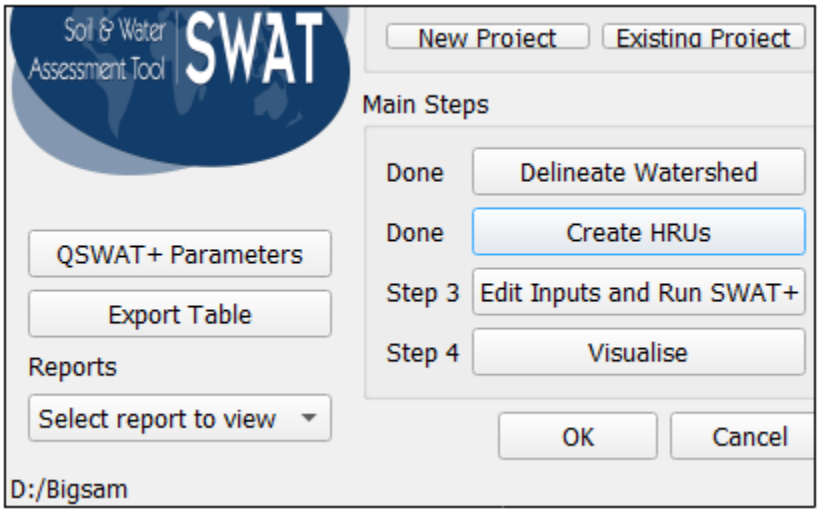

Figure 3.8 A display of the QSWAT+ model interface

The automatic watershed delineation procedure was then used to delineate the watershed, create its streams network, subbasins and landscape units as follows: firstly, the DEM was loaded onto the QSWAT+ model interface and the streams/channels were created. The streams network was then thoroughly inspected after which two outlet points were defined. These two outlets were then reviewed to confirm that they were successfully snapped before the watershed was created.

The LULC and soil maps, the lookup tables, the "usersoil" table and the slope bands were then added onto the QSWAT+ model interface and the HRUs were created, as shown in Figure 3.9. The attributes table of the "HRUs shapefile" was then opened and the cross-sectional areas of the HRUs were analysed. It was discovered that the majority of the HRUs created under the FRST, URBN, WATR, SWRN and WETL land uses had areas less than 0.1 hectares, which may not provide adequate catchments for RWH. For this reason, a threshold of 10, 10 and 2 per cent for land use, soil and slope, respectively, was applied to eliminate such HRUs. Consequently, the remaining number of HRUs were fairly manageable and they comprised of only three LULC classes, namely, RNGE, RNGB and AGRL (grasslands, shrublands and croplands), respectively.

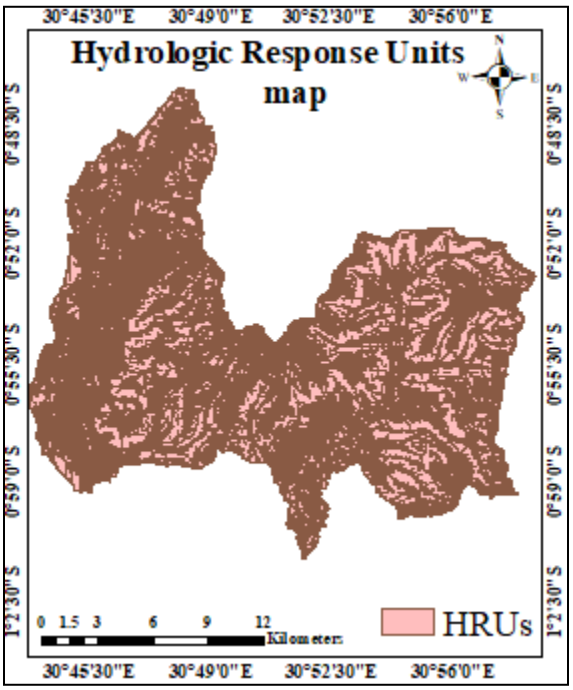

Figure 3.9 The HRUs map for the Bigasha watershed

The weather generator (which was downloaded together with the QSWAT+ software), weather stations information and daily observed weather data were then imported onto the SWAT+ editor interface. The SWAT+ editor is a specially designed interface for modifying the QSWAT+ model inputs and running the model. The purpose of the weather generator was to fill missing weather data and simulate weather parameters in parts of the Bigasha watershed that were located far away from Mbarara meteorological station. The simulation and warmup periods ({2000 – 2020} and 3 years, respectively) and the outputs to be printed and their temporal scales were then specified after which the QSWAT+ model was run to simulate the runoff from the Bigasha watershed.

Since this study was concerned with runoff simulation, the monthly and yearly runoff from the two outlet channels ("No. 55" and "No. 68") mentioned earlier and the annual average runoff depths from the HRUs were selected for visualisation of the results of the modelling process. The annual average runoff depths from the HRUs were later used to select potential sites for RWH in the Bigasha watershed, besides, computing the runoff volumes from those sites. Although the Bigasha watershed has two distinct rainfall seasons (MAM and SON), the average seasonal runoff depths from the HRUs could not be used to identify potential sites for RWH in this area. This is because there were inconsistencies in the onset and recession dates of the seasonal rainfalls across the years.

3.4.2 Model sensitivity analysis, calibration, validation and performance evaluation

This was performed with the help of SWATPlusCUP, which is the calibration program for the QSWAT+ model. Since the model was calibrated using the stream flow data from the Kagera river, the QSWAT+ model for the Kagera river basin (KRB) was first built. The calibration was performed in line with the protocol prescribed by Abbaspour et al. (2017).

3.4.2.1 Building of the KRB model and its SWATPlusCUP project

The steps undertaken to build the KRB model were the same as those followed while developing the Bigasha watershed model discussed earlier. The only difference here is in the sources of the input datasets particularly the soil, land use and climate data. The resampled soil map with 10 meters spatial resolution used in this model consists of 31 soil types and it was obtained from the FAO Digital Soil Map of the World (DSMW) database (Scale 1: 5 000 000). The land use map with eight LULC classes, like that of the Bigasha watershed LULC maps, was clipped from the open access global land cover map with a spatial resolution of 10 meters. This map was

downloaded from the European Space Agency (ESA-2020) database (Tsendbazar et al., 2021). The validated overall accuracy of the clipped map (using Google Earth Pro) was 92.7 per cent and the Kappa coefficient was 0.92, which is above the minimum acceptable LULC classification accuracy of 85 per cent proposed by Anderson et al. (1976).

Lastly, the global weather data, covering a period of 15 years (1999 – 2013), with no years of missing data, for the 11 weather stations that were identified within the KRB were downloaded from the Climate Forecast System Reanalysis (CFSR, for four stations) and the Climate Hazards Infrared Precipitation with Stations (CHIRPS, for seven stations) databases. The annual average rainfall recorded at each of the 11 weather stations stated above range from 700 – 2 000 mm, which is reported by Habiyakare & Zhou (2015) as the annual average rainfall distribution across the Kagera river basin. This explains why the climate data from the two databases were selected and used to build the KRB model.

There was only one outlet specified for the entire watershed. This outlet was drawn on the model's main channel located at a point close to the Kagera river gauging station at Masangano (latitude: 0° 56'21'' S, longitude: 31° 45' 48'' E and elevation: 1133.0 m above sea level). This was the only gauging station whose streamflow data was available at the Ministry of Water and Environment offices in Uganda. Since the Kagera river is a perennial river, it was expected that the above stream flow data would include base flow. However, the information on the source(s) of this base flow were not available and thus was not included during the modeling process.

That said, the base flow was separated from the observed daily stream flow as follows: at first, the base flow separation (filter) program developed by Arnold (1999) as cited by Haguma (2007) was used. However, after the filter had made the three passes through the daily stream flow records, it was discovered that the filter underestimated surface runoff as partially shown in Table 3.7. This was detected from the plotted graph of the estimated monthly surface runoff versus the simulated surface runoff (whose values are partially depicted in Table 3.7). The base flow estimates from the filter was about 93 per cent of the stream flow which agrees with the base flow estimates (of greater than 80 per cent) reported by Haguma (2007), from the use of the same filter in the KRB.

In the second approach, the constant base flow separation technique was also tested. Here, the long-term average low flow of the Kagera river of 85 m^3/s reported by Habiyakare & Zhou (2015)

was subtracted from the observed monthly stream flow records. The resultant observed monthly surface runoff values obtained from this approach were almost three times higher than those obtained from the base flow filter as partially shown in Table 3.7 below.

Table 3.7 Sample of the surface runoff estimates for the Kagera river

Year/month)	Base flow filter surface runoff estimates (m^3/s)	Constant threshold surface runoff estimates (m^3/s)	Simulated surface runoff (m^3/s)
2002/1	3.41	11.98	21.17
2002/2	8.37	30.41	13.77
2002/3	22.22	64.80	55.81
2002/4	31.36	105.13	119.40
2002/5	8.99	36.50	75.67

Moreover, there was a better agreement between the plotted graph of the observed monthly surface runoff obtained by the constant baseflow separation method and that of the simulated surface runoff. Therefore, this was the observed monthly surface runoff data that was used to calibrate and validate the KRB model runoff simulations for the 15-year period results (1999 – 2013). The calibration and validation data were partitioned with the understanding that the mean (standard deviation) of the two datasets were not significantly different from each other, that is to say, 16.70 (18.59) for calibration data and 17.26 (21.23) for validation data. This was done to ensure that during calibration and validation, all climate scenarios (wet, average and dry) were captured.

The new SWATPlusCUP project named “Kag12” was created in the SWATPlusCUP software interface, as shown in Figure 3.10. The KRB model simulation results were then imported onto the above project and the SWAT parameter estimator (SPE) was selected as the calibration algorithm. The model was calibrated for nine years (2005 – 2013), two of which (2005 – 2006) were set as the warm up period for the model while validation took six years (1999 – 2004), with three years (1999 – 2001) set as the warm up period as well.

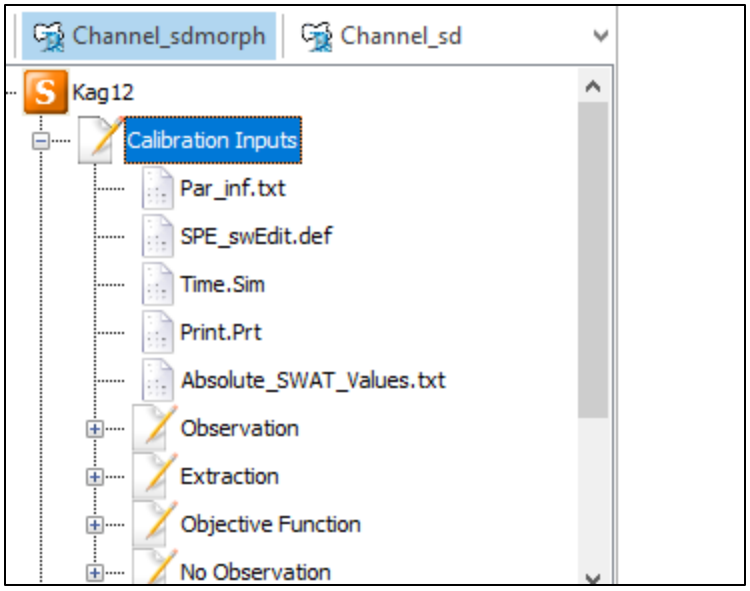

Figure 3.10 The SWATPlusCUP calibration program interface

3.4.2.2 Pre-calibration/initial model run in SWATPlusCUP

This was performed to check whether the developed model could be calibrated successfully. To achieve this, a dummy parameter "r_WDPQ.bsn...0...0" was first added to the "Kag12" project created. The simulation and printing periods for calibration of the model were then specified. The observed monthly surface runoff data for calibrating the model was then added to the above project. The simulated monthly surface runoff, for period corresponding to that of the calibration data, from the main outflow channel ("No.1") of the KRB was then selected for extraction. The Nash Sutcliffe efficiency (NSE) was then selected as the objective function type and the initial model run of one simulation was executed.

3.4.2.3 Parameter(s) identification and sensitivity analysis

Considering the behavior and performance of the initial model, 14 parameters listed in Table 3.8, were identified from previous studies by Abbaspour et al. (2007, 2017), Arnold et al. (2012), Cha et al. (2014) and Kouchi et al. (2017) for the calibration process.

Table 3.8 Selected parameters for model calibration

Parameter change	Description	Initial range	Calibrated value
r__GW_REVAP.gw	Groundwater "revap"/percolation coefficient	-0.5 – 0.5	-0.02173
r__GW_DELAY.gw	Groundwater delay	-0.8 – 0.8	-0.05932
r__SOL_K().sol	Saturated soil hydraulic conductivity	-0.8 – 0.8	-0.15274
r__SOL_AWC().sol	Available water capacity of the soil layer	-0.5 – 0.5	0.18058
r__CN2.mgt	SCS runoff curve number	-0.3 – 0.2	-0.12056
r__OV_N.hru	Manning's "n" value for overland flow	-0.4 – 0.5	-0.13405
r__HRU_SLP.hru	Average slope steepness	-0.5 – 0.4	-0.35059
r__SLSUBBSN.hru	Average slope length	-0.4 – 0.5	0.19574
r__ALPHA_BF.gw	Baseflow alpha factor	-0.8 – 0.8	0.70174
v__SURLAG.bsn	Surface runoff lag time	0.05 – 24	10.12326
r__REVAPMN.gw	Threshold depth of water in the shallow aquifer for "revap"/percolation to occur	-0.5 – 0.5	-0.48033
v__CANMX.hru	Maximum canopy storage	0 – 100	56.25000
r__SOL_BD().sol	Moist soil bulk density	-0.6 – 0.6	-0.15274
r__GWQMN.gw	Threshold depth of water in the shallow aquifer required for return flow to occur	-0.8 – 0.8	-0.24134

(Source: Arnold et al., 2012; Cha et al., 2014), where *v* and *r* are *value* and *per cent* changes.

CANMX.hru is a parameter that introduces water to the watershed (driving variable). For this reason, it was calibrated separately to minimise identifiability problems during calibration. To achieve this, the CANMX.hru parameter was added to the "Kag12" project and its absolute range (0 – 100) was set. Four simulations were then run and using results of the 'local" parameter sensitivity analysis, the value of CANMX.hru was fitted. The remaining 13 parameters were then calibrated. Initially, the parameters were added to the "Kag12" project and an iteration of 300 simulations was run, as recommended by Abbaspour (2021). A "global" parameter sensitivity analysis was then performed from which a decision was made to use all the 13 parameters in the subsequent parameter optimisation processes.

3.4.2.4 Model parameter optimisation and post processing

The outputs of the first iteration were visualised in this step, specifically the 95PPU graph and the values of the three objective functions/efficiency criteria, namely, the NSE, R^2 and PBIAS, which were used to assess the prediction accuracy of the KRB model. The "Multiple objective function" post processing option was used in this study to minimise parameter conditionality problems in

the calibrated model, as highlighted by Abbaspour et al. (2017). Since the SPE algorithm is iterative, the final calibrated model was obtained after four iterations, each of 300 simulations. The results of the "best simulation" after the fourth iteration were then used to assess the accuracy of the calibration as well as the goodness of the KRB model.

3.4.2.5 Model validation

The observed monthly surface runoff data for validating the KRB model's predictions was first added to the "Kag12" project. The simulation and printing periods for validation of the model were then specified. The simulated monthly surface runoff, for period corresponding to that of the validation data, from channel No.1 mentioned earlier was then selected for extraction. An iteration of 300 simulations was then run using the fitted parameters of the final calibrated model, as recommended by Abbaspour (2021). The results of the "best simulation" of the validated model were then used to evaluate the prediction accuracy of the KRB model.

Finally, 10 out of the 14 parameters, viz. GW_REVAP.gw, GW_DELAY.gw, SOL_K().sol, SOL_AWC ().sol, CN2.mgt, ALPHA_BF.gw, REVAPMN.gw, CANMX.hru, SOL_BD().sol and GWQMN.gw, used to calibrate and validate the KRB model were selected and used to calibrate the Bigasha watershed model, using the "NO observation" option of SWATPlusCUP. This was done because the Bigasha watershed does not have its own gauged outlet. The selected parameters were those that were believed to have influenced surface runoff simulation in Bigasha. It is at this point that the annual average runoff depths from the HRUs were extracted and used to estimate potential sites for RWH in the Bigasha watershed.

3.4.3 Rainwater harvesting site suitability analysis

The four commonly used RWH site suitability analysis criteria/factors, namely, topography (slope), soils, land use and rainfall and runoff depth (Ammar et al., 2016), were used to detect potential sites for RWH in the Bigasha watershed. The potential sites from each of the three LULC maps used in this study were selected from the HRUs with the highest runoff generating capacities. These HRUs were identified as follows: firstly, the *.txt file containing the extracted annual average runoff depths from the HRUs was opened. The contents of this file were then copied and pasted into a new Microsoft Excel worksheet. The columns with undesired information were then deleted from the worksheet leaving only those with the runoff depths ("surq_gen"), Unit IDs and HRUs names.

Similarly, the attributes table of the "HRUs shapefile" was opened in QGIS and its contents were copied and pasted into the same Excel worksheet mentioned above. The most relevant information from the contents of the attributes table were the HRUs areas, HRUs IDs, LULC classes and soil and slope categories. The column with the HRUs runoff depths ("surq_gen") was then selected and its values were sorted in descending order, as shown partially in Table 3.9, in the case of the 2022 LULC map.

Table 3.9 Sorted runoff depths from the HRUs of the 2022 LULC map

(*.txt) file information			**Attributes table information**				
Unit (IDs)	HRUs name	surq_gen (mm)	Land use	Soil	Slope band (%)	Area (ha)	HRUs (IDs)
330	hru330	120.964	RNGB	I-U-c-3132	0-5	0.39	330
347	hru347	120.781	RNGB	I-U-c-3132	0-5	0.41	347
689	hru689	119.362	RNGB	I-U-c-3132	0-5	0.54	689
134	hru134	116.605	RNGB	I-U-c-3132	0-5	1.1	134

The values of the sorted runoff depths from the HRUs, their contributing catchment areas and the respective land use, soil and slope categories were then thoroughly analysed. A decision was then made to select HRUs with an annual average runoff depth of at least 92 mm to constitute potential sites for RWH in the Bigasha watershed. This threshold was chosen because the runoff depths from the rest of the HRUs were less than 60 mm and thus would require large catchment areas to harvest adequate amount of rainwater from them.

The RWH site suitability maps obtained from the three LULC maps were generated using QGIS. This involved deleting the contents of the HRUs whose runoff depths were less than the 92 mm threshold, from the attributes table of the "HRUs shapefile" mentioned earlier. All three of the RWH site suitability maps were then validated using Google Earth Pro. Finally, the total volume of surface runoff that could be harvested from the potential RWH sites was computed as a summation of the individual runoff volumes harvestable from the selected HRUs, as illustrated by the equation below:

$$\text{Total volume of surface runoff} = \sum_{i=1}^{n} A_i * R_i \quad \text{.....(3.5)}$$

where *i* is the selected HRU number, A is the area of the i^{th} HRU and R is the runoff depth of the i^{th} HRU.

3.4.4 Determination of the irrigation water requirement of the coffee crop

This was calculated using the CROPWAT 8.0 software. The calculation was performed in three stages as follows: firstly, the monthly reference evapotranspiration (ET_o) for 18 years (2003 – 2020), was computed using the Penman-Monteith method. To achieve this, the monthly weather data for four out of the five climatic variables (relative humidity, minimum temperature, maximum temperature and wind speed) prepared earlier and the CROPWAT sunshine hours estimates were first added to the CROPWAT model. The model then computed both the monthly solar radiation and reference evapotranspiration automatically, as depicted graphically in Table 3.10, for the year 2003. The calculation was performed from 2003 – 2020 to match with the period when the QSWAT+ model simulations were printed.

Table 3.10 Monthly ET_o for the year 2003 calculated by the CROPWAT model

Month	Min Temp	Max Temp	Humidity	Wind	Sun	Rad	ETo
	°C	°C	%	m/s	hours	MJ/m²/day	mm/day
January	15.5	28.1	73	2.1	8.5	22.0	4.54
February	17.3	31.4	55	2.4	9.3	23.9	5.87
March	17.4	30.1	64	2.4	8.5	22.9	5.38
April	16.7	28.0	75	2.3	7.7	20.9	4.48
May	15.6	26.0	81	2.6	7.2	19.0	3.80
June	15.3	26.9	67	2.8	7.9	19.2	4.39
July	14.3	26.7	56	3.2	8.4	20.2	5.04
August	15.5	27.8	56	2.9	8.3	21.2	5.22
September	16.4	28.4	60	2.9	8.1	21.9	5.31
October	16.9	28.1	70	2.4	7.7	21.3	4.72
November	16.1	26.1	83	2.0	6.9	19.6	3.83
December	15.8	27.1	76	2.1	7.7	20.5	4.18

In order to incorporate the effects of climate variability and uncertainty on the resultant crop and irrigation water requirements, Weibull distribution analysis was conducted on the calculated ET_o values. In this analysis, the monthly ET_o values for the 18 years were first ranked in descending order and their respective probabilities of exceedance (POE) were calculated using the Weibull equation expressed as:

$$POE = 100 * \left(\frac{r}{N+1}\right) \quad \text{..... (3.6)}$$

where *r* represents the rank position while *N* stands for the number of events in the period of record, which was 216 months in this case.

The POE of 25 per cent threshold, which is close to the POE of 33 per cent, used for flood frequency analysis in hydrological studies was then selected. The ET_o corresponding to the POE selected above was later used to compute the crop water requirement of the coffee crop throughout the 18-year period studied. This ET_o was selected because it caters for high evapotranspiration rates whose resultant coffee crop and irrigation water requirements should be met by the harvestable rainwater at the Bigasha watershed. Consequently, coffee farmers' vulnerability to crop losses associated with such ET_os would be lessened.

The monthly precipitation data was added to the CROPWAT model in the second stage and the effective rainfall for the 18-year period was calculated. The USDA soil conservation service method, which is recommended for estimating effective rainfall in water scarce areas (Bokke & Shoro, 2020) such as the Bigasha watershed, was used in this study. Finally, the coffee crop information, namely, the length of crop growing stages, the crop coefficient (K_c), the critical depletion factor (p), the rooting depth (Z) and the yield response factor (K_y) were added to the CROPWAT model. The model then calculated both the decadal crop and net irrigation water requirements of the coffee crop automatically.

Coffee is a perennial crop which takes between three and four years before the first harvest. For this reason, the total growth season of the crop was distributed across the years, with each year taking 365 days in order to match with the yearly rainfall records. It is these 365 days that was divided among the four growth stages in the CROPWAT model, with each stage taking approximately 91 days. The planting date of the coffee crop was selected as 15th August so that the coffee plants benefit from the high SON seasonal rains during their flowering stage. Flowering of the coffee plant occurs usually at the start of the third year of its growth.

The resultant annual crop and net irrigation water requirements of the coffee crop for 18-year period were obtained by summing the respective decadal values calculated earlier. The annual average gross irrigation water requirement was then computed as a ratio of the annual average net

irrigation water requirement to the irrigation efficiency, assuming a drip irrigation system with an irrigation efficiency of 90 per cent was used.

3.4.5 Determination of the potential irrigable area under coffee

The total area of coffee fields that could be irrigated using the harvestable rainwater at the Bigasha watershed was computed from the ratio of the annual average volumes of surface runoff attainable from the potential sites derived from the 2022 LULC map to the annual average gross irrigation water requirement of the coffee crop as illustrated by the equation below:

$$\text{Irrigable coffee field} = \frac{\text{Annual average volume of rainwater harvestable from potential sites}}{\text{Annual average gross irrigation water requirement of coffee}} \quad ..(3.7)$$

The runoff volume attainable from the 2022 LULC map was chosen because it gives a better representation of the current conditions at the Bigasha watershed compared to those from the 2010 and 1999 LULC maps.

CHAPTER 4: RESULTS AND DISCUSSION

4.1 Potential RWH sites in the Bigasha watershed

The number of HRUs selected to constitute potential sites for RWH in the Bigasha watershed were 62, 125 and 114 out of the original 690, 720 and 995 HRUs that were derived from the 1999, 2010 and 2022 LULC maps, respectively. As highlighted in the methodology section, the above HRUs were those whose annual average runoff depths were greater than 92 mm. There was a high number of HRUs in the 720 HRUs category with potential for RWH. This may be attributed to the dominance of shrublands (which are good runoff generators) on the 2010 LULC map than the other two maps, as shown in Figure 4.1. The results of the RWH site suitability analysis performed in this study shows that the dominant land use, soil and slope at the selected potential RWH sites were shrublands (RNGB), Leptosols (I-U-c-3132) and >10 per cent slope, respectively, as summarised in Table 4.1 below.

Table 4.1 Summary of the dominant land use, soils and slope at the potential RWH sites

Year	Land use	Soil	Slope (%)	Total area (ha)	Runoff volume (MCM)
1999	RNGB	I-U-c-3132	> 10	1591	1.61
2010	RNGB	I-U-c-3132	>10	2596	2.68
2022	RNGB	I-U-c-3132	>10	1327	1.39

Shrublands are often characterised by sparsely distributed vegetation that offer minimal interception to precipitation and thus is capable of generating high surface runoff. However, it is important to note that grasslands were the most dominant LULC class in the Bigasha watershed, accounting for 78, 73 and 59 per cent of the 1999, 2010 and 2022 LULC maps, respectively, as shown in Figure 4.1. This was already an indication that the majority of the Bigasha watershed's area could be poor runoff generators and hence have low potential for rainwater harvesting. According to Jia et al. (2020), the presence of surface vegetation on grasslands interferes with runoff generation by increasing surface roughness to runoff, lengthening the runoff flow path and increasing the soil's infiltration capacity through the rooting system of the vegetation.

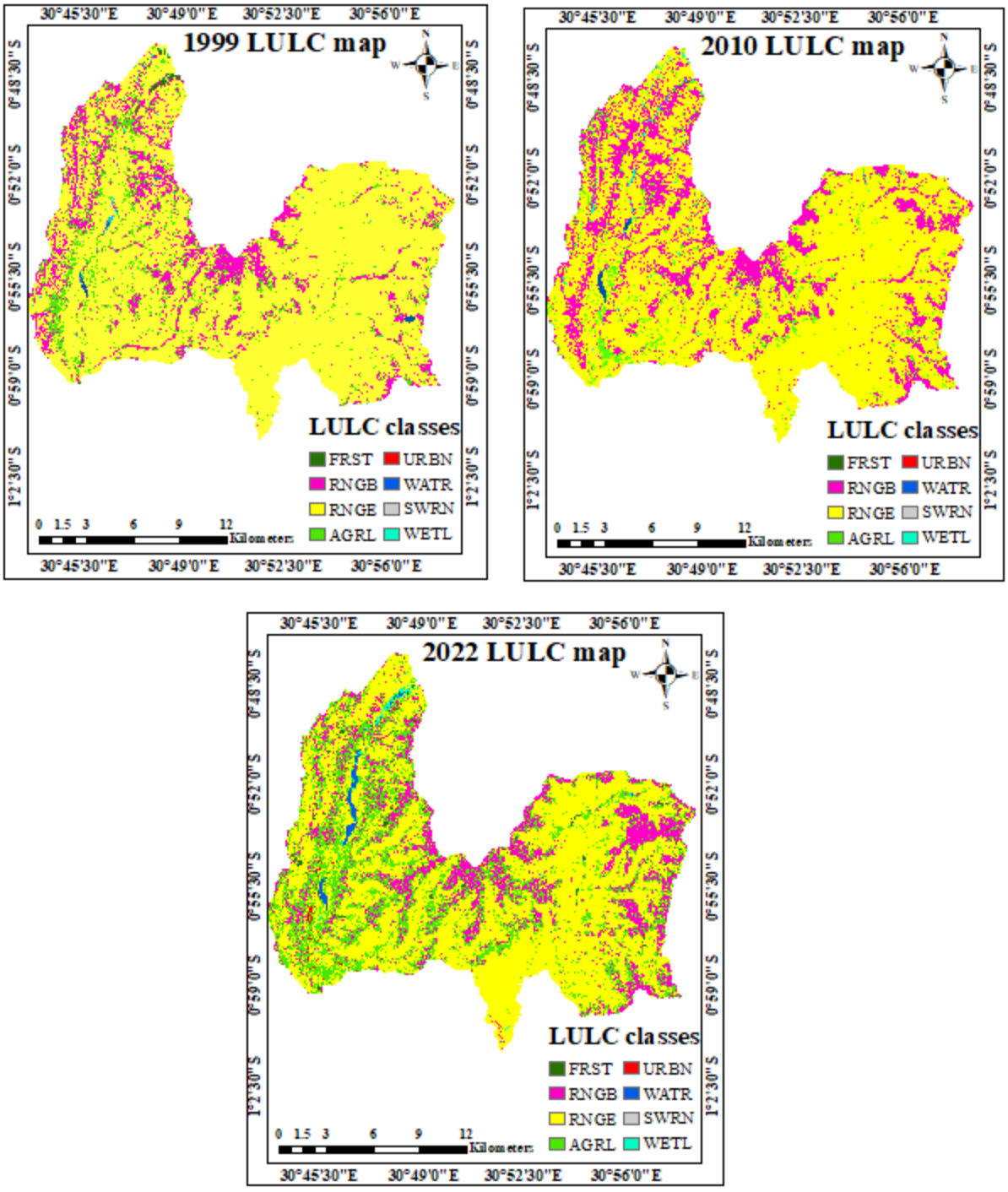

Figure 4.1 The 1999 – 2022 LULC maps for the Bigasha watershed

NB: The overall classification accuracies of the three LULC maps shown above were 92.5, 96.7 and 94.0 per cent, for the 1999, 2010 and 2022 maps, respectively, all of which are above the minimum acceptable accuracy of 85 per cent proposed by Anderson et al. (1976).

The estimated potential sites were dominated by Leptosols because these are moderately fine to fine-textured soils with low infiltration rates and thus good runoff generators. The Leptosols (I-U-c-3132) soil type found in the Bigasha watershed are hydrologic soil group (HSG) C soils. Maidment et al. (1993) indicated that HSG C soils have low infiltration rates when thoroughly wetted and their layers impede downward movement of water. As shown in Figure 4.2, HSG C soils (Leptosols and Orthic Ferralsols) cover up to 76 per cent of the Bigasha watershed's total land area. However, the majority of these areas may be unsuitable for RWH. This is because the predominant land uses in the aforementioned areas are grasslands and croplands, which have poor runoff generating characteristics.

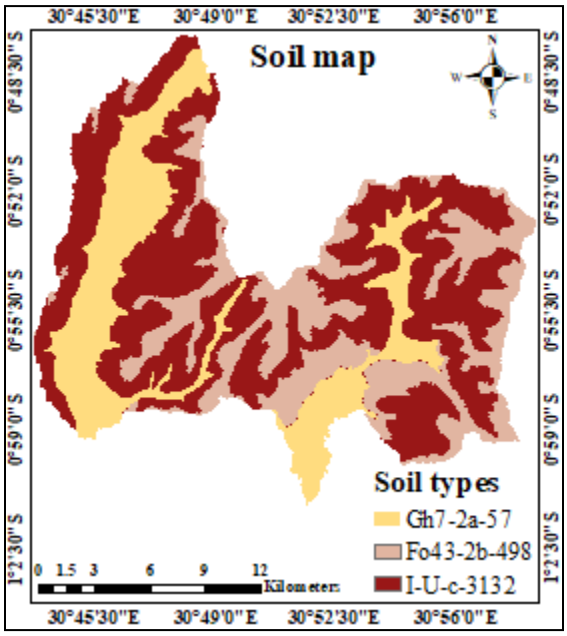

Figure 4.2 The soil map for the Bigasha watershed

As expected, the potential RWH sites were identified in areas with slope greater than 10 per cent. This is because such steep slopes are characterised by fast flowing surface runoff which reduces the time the water needs to infiltrate into the soil (Al-Ghobari & Dewidar, 2021). However, such slopes are more susceptible to erosion and necessitate extensive earthworks to install a RWH structure. Ideally, areas with slopes less than 5 per cent, that occupied 17 per cent of the Bigasha watershed, as shown Figure 4.3 would be potential sites for rainwater harvesting. However, this is not the case because the majority of the above-mentioned areas are covered by grasslands and Humic Gleysols, both of which have poor runoff generating characteristics.

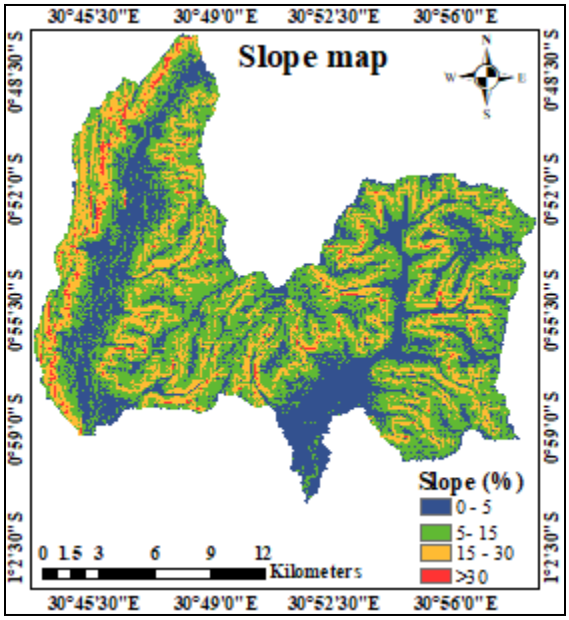

Figure 4.3 The slope map for the Bigasha watershed

There was no analysis carried out to compare the spatial distribution of the selected potential RWH sites and the rainfalls received in the Bigasha watershed. This is because this study relied on point rainfall data from a single meteorological station (Mbarara). Nonetheless, the annual average rainfall received in the Bigasha watershed over the 21-year study period was 954 mm, which falls within the FAO recommended range of 100 – 1 000 mm annual rainfall for RWH (Nyirenda et al., 2021).

Figure 4.4 depicts the three RWH site suitability maps that were developed. When these maps were overlaid on Google Earth Pro, it was confirmed that the predicted potential RWH sites fell in areas that are dominated by shrublands and hilly terrains as previously discussed. Therefore, there is sufficient evidence to accept the argument made by Ammar et al. (2016) that integrating remote sensing, GIS and hydrological models provides an accurate method for RWH site selection.

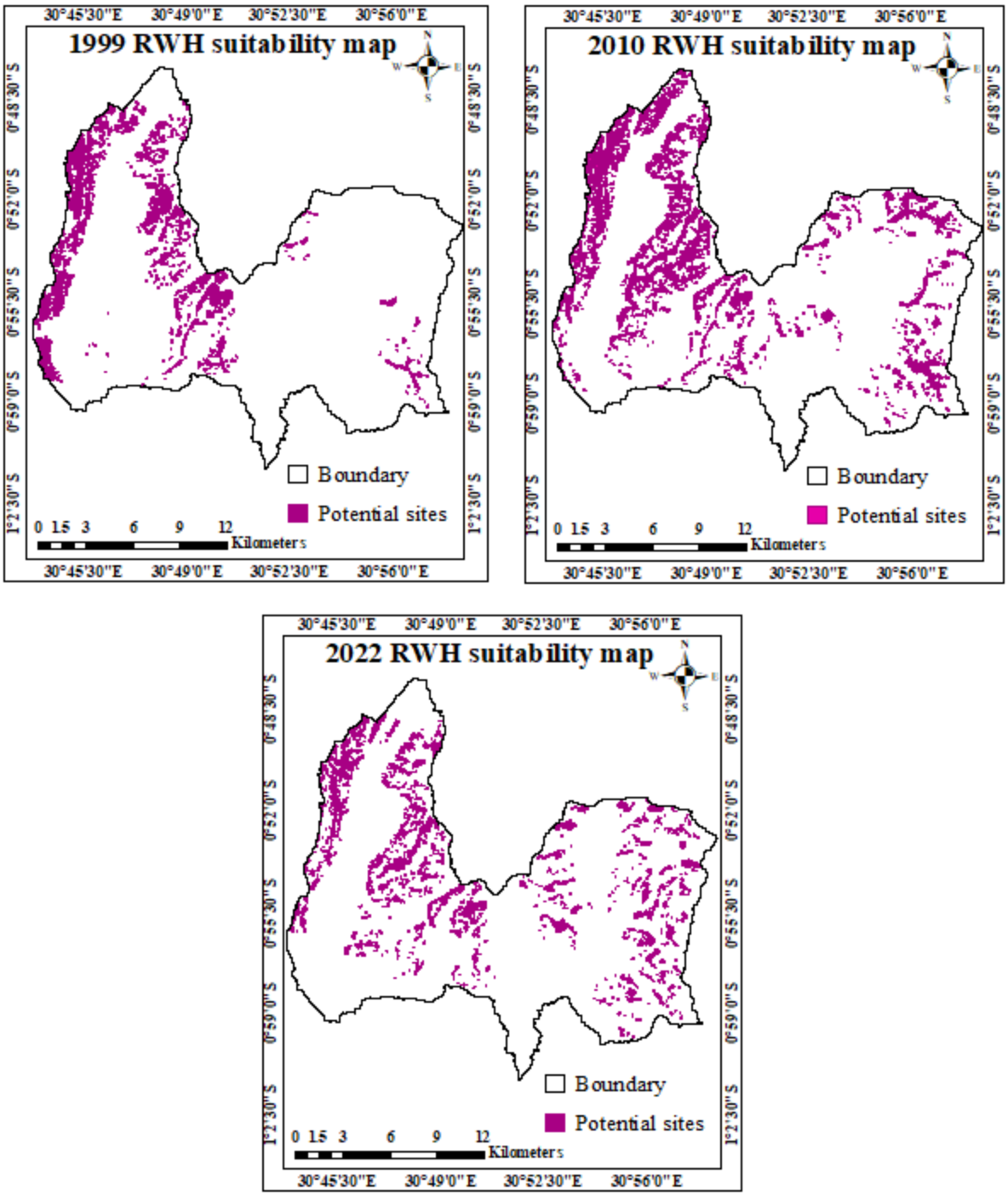

Figure 4.4 The 1999 – 2022 RWH suitability maps for the Bigasha watershed

4.2 Harvestable rainwater from the potential sites

The potential RWH sites estimated by the 125 HRUs created from the 2010 LULC map were capable of generating the highest total annual average surface runoff volume of 2.68 million cubic meters (MCM), from a catchment area of 2 596 ha. On the other hand, the potential sites identified

by the 114 HRUs created from the 2022 LULC map had the lowest total annual average surface runoff volume of 1.39 MCM harvestable from an area of 1 327 ha. In other words, the amount of rainwater that could currently potentially be harvested from the Bigasha watershed is 1.39 MCM. In summary, at least 2.8 per cent (1 000 ha) of the Bigasha watershed's total land area of 34 793 ha is suitable for rainwater harvesting, as shown in Table 4.1.

One would expect the potential RWH sites identified by the 62 HRUs created from the 1999 LULC map, which had the lowest number of HRUs with potential for RWH to generate the least amount of surface runoff. However, this was not the case because the 62 HRUs occupied a larger catchment area of 1 591 ha which is higher than that occupied by the 114 HRUs. The total annual average surface runoff harvestable from the 62 HRUs category was 1.61 MCM. Thus, the assumption that potential RWH sites with the highest number of HRUs have the greatest amount of surface runoff available is sometimes misleading.

In fact, this was the reason why undesired HRUs were eliminated from the Bigasha watershed model as indicated in the methodology section. Another significant finding was that the simulated annual average surface runoff from channel "No.68" (the Bigasha river) was 0.54 m^3/s in 2011 and 2012. This figure corresponds to the 0.5 m^3/s annual average surface runoff recorded by Droogers et al. (2012) from the Bigasha river between February 2011 and May 2012. It should be recalled that above mentioned records were made as part of the Nile Basin Initiative irrigation potential assessment project for the Bigasha watershed. The above observation therefore provides enough evidence to conclude that the simulated surface runoff from the Bigasha watershed is reliable and hence justifying the effectiveness of the QSWAT+ model for runoff simulation.

4.3 Performance of the Kagera river basin (KRB) model

The results of the three statistical indices (efficiency criteria), namely, NSE, R^2 and PBIAS, which were used to assess the performance of the calibrated and validated model for the KRB are shown in Table 4.2. Similarly, the plotted "SWAT Graph" of the observed monthly surface runoff data versus the simulated runoff of the calibrated and validated model is shown in Figure 4.5.

Table 4.2 Summary of the performance of the KRB model

Performance index	Calibrated value	Validated value	Acceptable value
NSE	0.81	0.87	> 0.5
R^2	0.82	0.88	>0.5
PBIAS (per cent)	0.4	8.7	0 ± 25

(Source: (Moriasi et al., 2007; Abbaspour et al., 2015; Amin & Nuru, 2020)

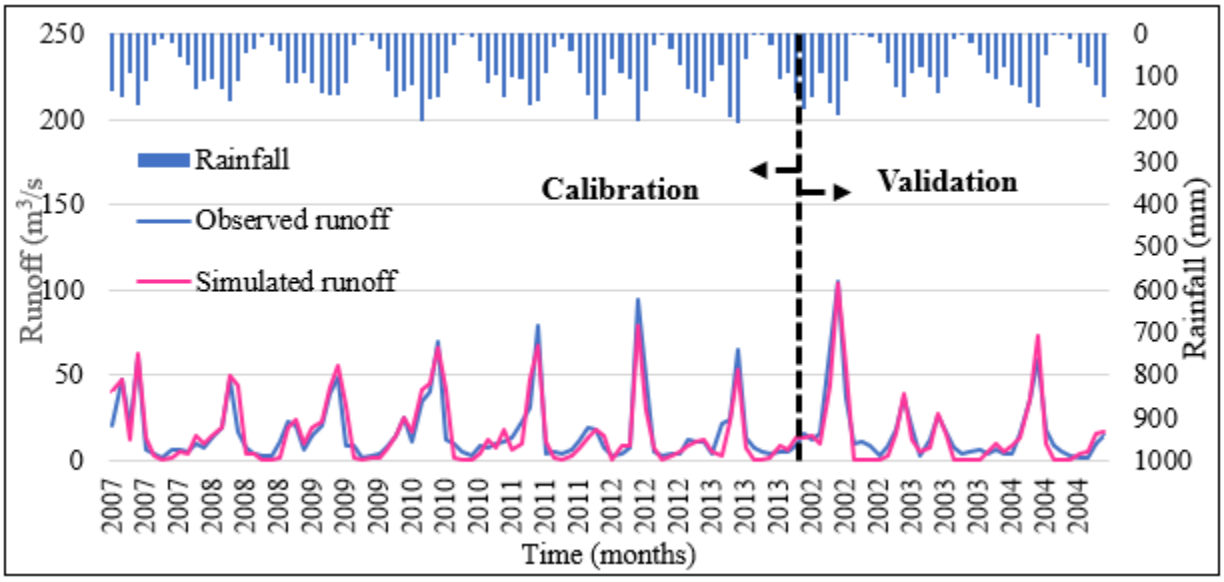

Figure 4.5 SWAT graph of the calibrated and validated model of the KRB

Generally, the overall performance of the KRB model was "very good" when compared to the acceptable performance ranges shown in Table 4.2. The model correctly predicted/bracketed a reasonable percentage of the Kagera river stream flow data with NSE(R^2) values of 0.81(0.82) and 0.87(0.88) obtained during calibration and validation, respectively. The above prediction accuracy is consistent with those reported in the studies conducted in different parts of the world by Harka et al. (2020), Li et al. (2020) and Adeogun & Sanni (2019) using various versions of the SWAT model. Therefore, the QSWAT+ model is not only an effective and reliable tool for surface runoff simulation, as highlighted by Bieger et al. (2017), but also for selecting suitable RWH sites.

4.4 Reference evapotranspiration, crop and irrigation water requirements of coffee

The monthly reference evapotranspiration rates computed by CROPWAT model at the Bigasha watershed range from 3.49 to 6.67 mm/day. The ET_o that was used for computing the crop and net irrigation water requirements of the coffee crop over the 18-year study period was 4.76 mm/day. It should be recalled that the above ET_o, which had a POE of 25 per cent, accounted for high ET_os whose resultant irrigation water requirements should be met by the harvestable rainwater at the Bigasha watershed. This would safeguard coffee farmers from risks of crop losses associated with such high ET_os.

The annual average effective rainfall and crop and net irrigation water requirements of the coffee crop computed by the CROPWAT model were 772 mm, 1 632 mm and 860 mm, respectively. The above crop water requirement lies within the range of 1 200 – 1 800 mm of water required annually for coffee grown in Uganda (UCDA, 2019), hence justifying the effectiveness of the CROPWAT model for irrigation water requirement calculations. Figure 4.6 shows the bar charts for the decadal crop and net irrigation water requirements of the coffee crop generated by the CROPWAT model for the year 2020.

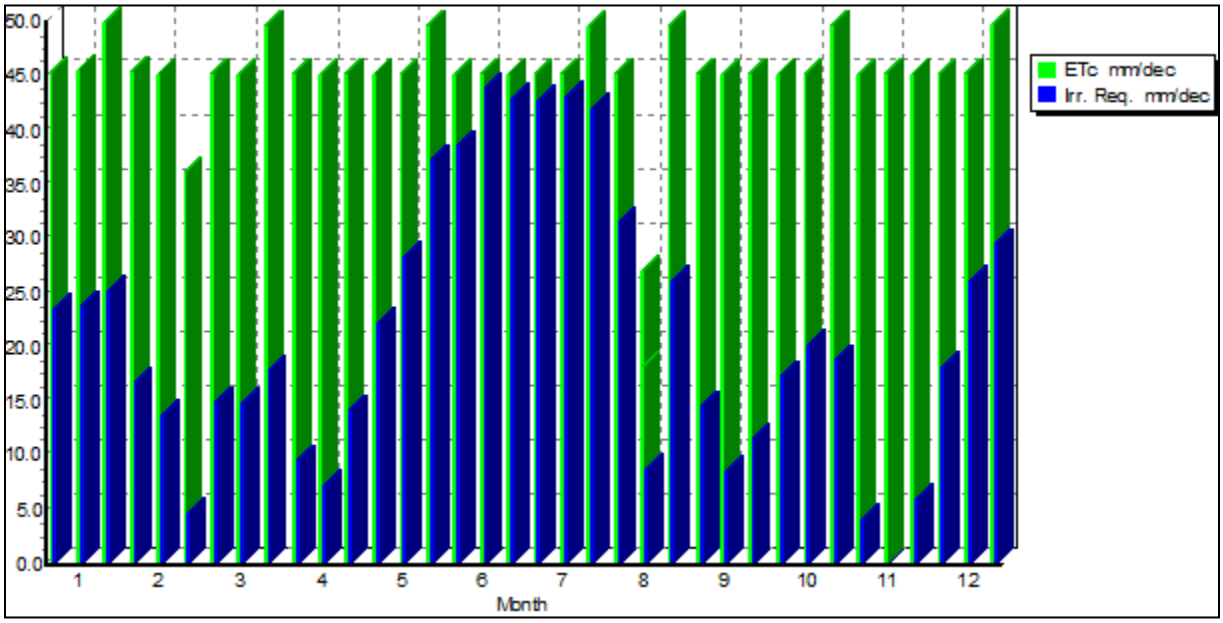

Figure 4.6 The calculated decadal crop and net irrigation water requirements

4.5 Potential irrigable area under coffee

The total area of the coffee fields that could be irrigated annually with the harvestable rainwater from the Bigasha watershed was calculated to be 145 ha. This figure was calculated using an annual average surface runoff volume of 1.39 MCM (harvestable from the 2022 LULC map), which provides a more accurate representation of the current conditions within the Bigasha watershed), an annual average gross irrigation water requirement of 955 mm and an irrigation efficiency of 90 per cent (assuming the drip irrigation system was used). The 145 ha represents 1.8 per cent of the current crop production area in the Bigasha watershed and 0.4 per cent of the entire watershed.

Therefore, it could be concluded that RWH for irrigated coffee farming could expand the current land under coffee production in the Bigasha watershed by up to 101.8 per cent. This area could be expanded even further by converting the grasslands found in parts of the Bigasha watershed, that have Leptosols/Orthic Ferralsols and slope less than 5 per cent, to shrublands. This is because as seen in the RWH site selection section, the 2010 LULC map, which had more shrublands as potential sites than the 2022 LULC map, generated twice as much surface runoff as the latter.

CHAPTER 5: CONCLUSION AND RECOMMENDATIONS

5.1 Conclusion

- Since the potential RWH sites that were identified from all three of the LULC maps are in areas that are dominated by a combination of shrublands, Leptosols and >10 per cent slope, it could be concluded that landscapes with such characteristics are best suited for RWH. However, the current potential for RWH in the area could have been reduced by grasslands and croplands (poor runoff generators), which occupy 82 per cent of the watershed.
- It turned out that the 125 HRUs that were created from the 2010 LULC map could generate the highest volume of harvestable rainwater (2.68 MCM) while the 114 HRUs that were created from the 2022 LULC map had the lowest runoff generating potential (of 1.39 MCM). This is because the 125 HRUs covered a land area that was almost twice as large as that covered by the 114 HRUs.
- It can be inferred that RWH for irrigated coffee farming could increase the current cropped area and the cropped area under coffee in this watershed by up to 1.8 and 101.8 per cent, respectively, since the estimated potential RWH sites are located in none cropland areas.
- Considering the high prediction accuracy of the KRB model with NSE(R^2) values of 0.81(0.82) for calibration and 0.87(0.88) for validation, it could be concluded that the QSWAT+ model is an effective and reliable tool for simulating surface runoff and thus estimating potential sites for rainwater harvesting.
- Finally, based on the overall land use land cover classification accuracy assessment results of 92.5, 96.7 and 94.0 per cent, obtained from the 1999, 2010 and 2022 LULC maps, respectively, created and used in this study, it can be concluded that the integration of the semi-automatic classification plugin and the K-nearest neighbor algorithm provides an effective tool for LULC classification.

5.2 Recommendations

The following recommendations are made from the study:

- Field visits to the identified potential RWH sites should be conducted to ascertain whether the model results are reliable.
- Silt and sediment traps should be installed at the future RWH reservoirs to minimise problems of soil erosion since the majority of the estimated potential RWH sites are located in hilly areas.
- Hydrological data collection in the Bigasha watershed (especially the flow data) should be enhanced for future use during validation of models that utilise such data.
- An analysis may be conducted to compare the spatial distribution of the identified potential RWH sites with rainfalls received in different parts of the Bigasha watershed.
- A detailed irrigation suitability study should be conducted in the Bigasha watershed to assess whether all the 145 ha of coffee fields determined from this study could actually be irrigated.
- The grasslands found in parts of the Bigasha watershed, that have Leptosols/Orthic Ferralsols and slope less than 5 per cent, may be converted to shrublands to increase the potential of RWH in this area.
- Remote sensing, GIS and the QSWAT+ model may be used to assess the potential of rainwater harvesting in other water stressed parts of Uganda since the QSWAT+ model has a reliable runoff prediction accuracy.

REFERENCES

Abbaspour, K.C., Rouholahnejad, E., Vaghefi, S., Srinivasan, R., Yang, H. & Kløve, B. (2015). A continental-scale hydrology and water quality model for Europe: Calibration and uncertainty of a high-resolution large-scale SWAT model. Journal of Hydrology, 524(2015), 733-752.

Abbaspour, K.C., Vaghefi, S.A. & Srinivasan, R. (2017). A guideline for successful calibration and uncertainty analysis for soil and water assessment: A review of papers from the 2016 international SWAT conference. Water (Switzerland), 10(6),1-18.

Abbaspour, K.C., Yang, J., Maximov, I., Siber, R., Bogner, K., Mieleitner, J., Zobrist, J. & Srinivasan, R. (2007). Modelling hydrology and water quality in the pre-alpine/alpine Thur watershed using SWAT. Journal of Hydrology, 333(2),413-430.

Abbaspour, K.C. (2021). SWATCUP-2019, SWATCUP-Premium and SWATCUP-Plus: SWAT Calibration and Uncertainty Programs. A User Manual. 2021, 1-69.

Abdulla, F. A. & Al-Shareef, A.W. (2009). Roof rainwater harvesting systems for household water supply in Jordan. Desalination, 243(1-3), 195-207.

Adane, A. & Bewket, W. (2021). Effects of quality coffee production on smallholders' adaptation to climate change in Yirgacheffe, Southern Ethiopia. International Journal of Climate Change Strategies and Management, 13(4-5), 511-528

Adeogun, B.K. & Sanni, I.M. (2019). Hydrological Modelling of Kangimi Dam Watershed using GIS and SWAT Model. International Journal of Engineering, 17(2019), 165-171.

Aghaloo, K. & Chiu, Y.R. (2020). Identifying optimal sites for a rainwater-harvesting agricultural scheme in iran using the best-worst method and fuzzy logic in a GIS-based decision support system. Water (Switzerland), 12(1913), 1-24.

Aish, A., Ayesh, K. & Al-Najar, H. (2021). Modelling of long-term effects of climate change on irrigation water requirement in the Gaza Strip, Palestine. Arabian Journal of Geosciences, 14(650), 1-8.

Ajibade, T.F., Nwogwu, N.A., Ajibade, F.O., Adelodun, B., Idowu, T.E., Ojo, A.O., Iji, J.O., Olajire, O.O. & Akinmusere, O.K. (2020). Potential dam sites selection using integrated techniques of remote sensing and GIS in Imo State, Southeastern, Nigeria. Sustainable Water Resources Management, 6(57), 1-16.

Akoyi, K.T. & Maertens, M. (2018). Walk the Talk: Private Sustainability Standards in the Ugandan Coffee Sector. Journal of Development Studies, 54(10), 1792-1818. 10.

Al-Ghobari, H. & Dewidar, A.Z. (2021). Integrating GIS-based MCDA techniques and the SCS-CN method for identifying potential zones for rainwater harvesting in a semi-arid area. Water (Switzerland), 13(704), 1-16.

Al-komaim, M.D.A., Fraiture, C., Aklan, M. & Lammeren, R. (2018). Site suitability analysis for different indigenous rainwater harvesting systems. A Case study of Sana ' a water basin, Republic of Yemen, Msc. thesis, Wageningen University and Research, Netherlands, 1-88.

Al-Ruzouq, R., Shanableh, A., Yilmaz, A.G., Idris, A.E., Mukherjee, S., Khalil, M.A. & Gibril,

M.B.A. (2019). Dam site suitability mapping and analysis using an integrated GIS and machine learning approach. Water (Switzerland), 11(1880), 1-17.

Alejo, L.A., Ella, V.B., Lampayan, R.M. & Delos Reyes, A.A. (2021). Assessing the impacts of climate change on irrigation diversion water requirement in the Philippines. Climatic Change, 165(58), 1-17.

Allen, R.G., Pereira, L.S., Reas, D. & Smith, M. (1998). Crop Evapotranspiration (guidelines for computing crop water requirements). Food and Agricultural Organisation Irrigation and Drainage Paper No.56, Rome, Italy,1-326.

Amin, A. & Nuru, N. (2020). Evaluation of the performance of SWAT Model to simulate stream flow of Mojo river watershed: In the upper Awash river basin in Ethiopia. Journal of Hydrology, 8(1), 7-18.

Ammar, A., Riksen, M., Ouessar, M. & Ritsema, C. (2016). Identification of suitable sites for rainwater harvesting structures in arid and semi-arid regions : A review. International Soil and Water Conservation Research, 4(2016), 108-120.

Anderson, R.J., Hardy, E.E., Roach, T.J. & Witmer, R.R. (1976). A Land Use And Land Cover Classification System For Use With Remote Sensor Data, Fourth edition, US Government Printing Office, Washington, 1-34.

AQUASAT. (2022). AQUASTAT - Food and Agriculture Organisations' Global information System on Water and Agriculture, The WaPOR database.

Arnold, J.G. & Allen, P.M. (1999). Automated methods for estimating base flow and ground water recharge from stream flow records. Journal of the American Water Resources Association, 35(2), 411-424.

Arnold, J.G., Allen, P.M., Muttiah, R. & Bernhardt, G. (1995). Automated base flow separation and recession analysis techniques. Ground Water, 33(6), 1010–1018.

Arnold, J.G., Kiniry, J.R., Srinivasan, R., Williams, J. R., Haney, E.B. & Neitsch, S.L. (2012). Soil & Water Assessment Tool Input/Output Documentation Version 2012. Texas Water Resource Institute, 1-649.

Arnold, J.G., Moriasi, D.N., Gassman, P.W., Abbaspour, K.C., White, M.J., Srinivasan, R., Santhi, C., Harmel, R.D., Van Griensven, A., Van Liew, M.W., Kannan, N. & Jha, M.K. (2012). SWAT: Model use, calibration, and validation. Transactions of ASABE, 55(4),1491-1508.

Bakir, M. & Xingnan, Z. (2008). GIS and remote sensing applications for rainwater harvesting in the Syrian Desert (Al-Badia). Twelfth International Water Technology Conference, IWTC12 2008 Alexandria, Egypt, 1-10.

Bandi, A., Rao, Y.R.S. & Kumar, S. (2020). Rainfall Runoff Modelling in Ephemeral River Basin Using SWAT. Journal of critical reviews, 7(13), 1589-1597.

Barron, J., Calfoforo, J., Cortesi, L., König, K.W., Malmer, A., Prasad, E. & Sharma, B. (2009). Rainwater harvesting: A life line for human well-being. A report for the United Nations Environment Programme and Stockholm Environment Institute, Nairobi, Kenya, 1-80.

Bettili, L., Pek, E. & Salman, M. (2019). A decision support system for water resources management: The case study of Mubuku irrigation scheme, Uganda. Sustainability (Switzerland), 11(6260), 1-19.

Bhowmick, P., Mukhopadhyay, S. & Sivakumar, V. (2014). A review on GIS based Fuzzy and Boolean logic modelling approach to identify the suitable sites for Artificial Recharge of Groundwater. Scholars Journal of Engineering and Technology, 2(3A), 316-319.

Bieger, K., Arnold, J.G., Rathjens, H., White, M.J., Bosch, D.D., Allen, P.M., Volk, M. & Srinivasan, R. (2017). Introduction to SWAT+, A Completely Restructured Version of the Soil and Water Assessment Tool. Journal of the American Water Resources Association, 53(1), 1-16.

Bokke, A.S. & Shoro, K.E. (2020). Impact of effective rainfall on net irrigation water requirement: The case of Ethiopia. Water Science, 34(1), 155-163.

Bunn, C., Lundy, M., Läderach, P., Fernández-Kolb, P. & Castro-Llanos, F. (2019). Climate-smart coffee in Uganda. International Center for Tropical Agriculture (CIAT), Cali, Colombia. Feed the Future, 1-24.

Cha, Y., Park, S.S., Kim, K., Byeon, M. & Stow, C.A. (2014). Water resources of the Black Sea Basin at high spatial and temporal. Water Resources Research, 10(1002), 5375-5377.

Chowdhury, M. & Paul, P.K. (2021). Identification of suitable sites for rainwater harvesting using fuzzy AHP and fuzzy gamma operator: a case study. Arabian Journal of Geosciences, 14(585), 1-19.

Cloke, H.L. & Schaake, J.C. (2020). Handbook of Hydrometeorological Ensemble Forecasting. In Handbook of Hydrometeorological Ensemble Forecasting. https://doi.org/10.1007/978-3-642-40457-3

Congalton, R.G. (1991). A review of assessing the accuracy of classifications of remotely sensed data. Remote Sensing of Environment, 37(1), 35-46.

Congedo, L. (2021). Semi-Automatic Classification Plugin Documentation. August Release 7.9.5.1, User Mannual, 1-231.

Dhami, B.S. & Pandey, A. (2013). Comparative review of recently developed hydrologic models. Journal of Indian Water Resources Society, 33(3), 34-42.

Dile, Y., Srinivasan, R. & George, C. (2022). QGIS Interface for SWAT+: QSWAT+Step by Step Setup for the Robit Watershed, Lake Tana basin Ethiopia, Version 2.2, March Issue, 1-137.

Diriba, B.T. (2021). Surface runoff modeling using SWAT analysis in Dabus watershed, Ethiopia. Sustainable Water Resources Management, 7(96), 1-11.

Dong, Q. (2018). Study on the Crop Irrigation Water Requirement Based on Cropwat in Jinghuiqu Irrigation Area. IOP Series: Materials Science and Engineering, 394 (022037), 1-7.

Doorenbos, J., Kassam, A.H., Bentvelsen, C. & Uittenbogaard, G. (1979). Yield response to water. Food and Agricultutal Organisation of the United Nations, Irrigation and Drainge paper 33, Rome, 1-203.

DPU. (2015). Isingiro District Local Government Five Year District Local Government Development Plan II 2015/2016-2019/2020, March Report, Republic of Uganda, 1-450.

Droogers, P., Nkurunziza, P., Bastiaanssen, W.G.M., Immerzeel, W.W., Terink, W., Hunink, J.E., Meijninger, W., Hellegers, P., Chevalking, S., Steenbergen, F. & Brandsma, J.B. (2012). Assessment of the Irrigation Potential in South Sudan, Tanzania and Uganda, Future Water Final Report, Nile Basin Initiative Project, 114(0) 1-204.

Droogers, P., Terink, W., Brandsma, J. & Immerzeel., W.W. (2011). Assessment of the Irrigation Potential in Burundi, Eastern DRC, Kenya, Rwanda, Southern Sudan, Tanzania and Uganda. Future Water Inception Report, Nile Basin Initiative Project, 100(0) 1-128.

Durodola, O.S., Bwambale, J. & Nabunya, V. (2020). Using every drop: Rainwater harvesting for food security in Mbale, Uganda. Water Practice and Technology, 15(2), 295-310.

Dwiatmojo, H.R., Ramelan, A.H. & Priyanto, E. (2021). Mapping of rain water harvesting potential at Keduang Sub-watershed, Central Java, Indonesia. IOP Conference Series: Earth and Environmental Science, 824(012029), 1-11.

Efthimiou, N. (2018). Hydrological simulation using the SWAT model: the case of Kalamas River catchment. Journal of Applied Water Engineering and Research, 6(3), 210-227.

FAO. (2015). National Investment Profile Water for Agriculture and Energy, Uganda. Food and Agriculture Organisation of the United Nations, 1-36.

Farooq, S., Kausar, R., Ashraf, A. & Haider, B. (2020). Exploring Surface Runoff Potential and Water Harvesting Sites in Dera Ismail Khan Rod-kohi Area Using GIS and Remote Sensing. Pakistan Academy of Sciences, 57(2), 1-10.

Farzana, S.Z., Zafor, M.A.Z. & Shahariar, J.A.S. (2019). Application of SWAT Model for Assessing Water Availability in Surma River Basin. Journal of the Civil Engineering Forum, 5(1), 29-38.

Feng, Z., Liu, D. & Zhang, Y. (2007). Water requirements and irrigation scheduling of spring maize using GIS and CropWat model in Beijing-Tianjin-Hebei region. Chinese Geographical Science, 17(1), 56-63.

Gabr, M.E. (2021). Modelling net irrigation water requirements using FAO-CROPWAT 8.0 and CLIMWAT 2.0: a case study of Tina Plain and East South ElKantara regions, North Sinai, Egypt. Archives of Agronomy and Soil Science, 00(00), 1-16.

Ganole, K. (2010). GIS-based surface irrigation potiean assessment of a river catchment for Irrigation development in Dale Woreda, Sidima zone SNNP. Msc.thesis, Haramaya University, Ethopia, 1-120.

Gayathri, K., Ganasri, B.P. & Dwarakish, G.S. (2015). A Review on Hydrological Models. International Conference on Water Resources, Coastal and Ocean Engineering (ICWRCOE 2015). Aquatic Procedia, 4(12), 1001-1007.

Ghanem, H.M.H., Jaramillo, C.F., Vasquez, E.J.I., Sara, J.J., Tovey, S.C., Izzi, G. & Nattabi, H. (2020). International Development Association Project Appraisal Document, Uganda Irrigation for Climate Resilience Project, Republic of Uganda, 1-101.

Gliński, J., Lipiec, J. & Stępniewski, W. (2008). Encyclopedia of Soil Science. Encyclopedia of Earth Sciences Series. Springer, Ward Chesworth University of Guelph, Canada, 1-860.

Habiyakare, T. & Zhou, N. (2015). Water Resources Conflict Management of Nyabarongo River and Kagera River Watershed in Africa. Journal of Water Resource and Protection, 7(12), 889-896.

Haguma, D. (2007). Development of a hydrologic model of Kagera River basin using remote sensing data. Msc.thesis, UNESCO-IHE, Institute for Water Education, Netherlands, 1-126.

Hakorimana, F. & Akcaoz, H. (2019). The Relationship between Coffee and Climate Factors: Case of Rwanda. Turkish Journal of Agriculture-Food Science and Technology,7(9), 1367-1376.

Harka, A.E., Roba, N.T. & Kassa, A.K. (2020). Modelling rainfall runoff for identification of suitable water harvesting sites in Dawe River watershed, Wabe Shebelle River basin, Ethiopia. Journal of Water and Land Development, 47(12), 186-195.

Hatibu, N. & Mahoo, H. (1999). Rainwater harvesting technologies for agricultural production : A case for Dodoma , Tanzania. Conservation tillage with animal traction, Animal Traction Network for Eastern and Southern Africa (ATNESA), 161-171.

Ibraimo, N. & Munguambe, P. (2007). Rainwater Harvesting Technologies for Small Scale Rainfed Agriculture in Arid and Semi-arid Areas. University of Eduardo, Mozambique, 1-41.

ICO. (2019). International Coffee Organisation, Country Coffee profile: Uganda. International Coffee Council, Nairobi, Kenya, 1-47.

ICO. (2022). Coffee prices readjust whilst Certified Stocks grow, Coffee Merket Report, March Issue, Internationnal Coffee Organisation, 1-10.

Arnold, J.G., Moriasi, D.N., Gassman, P.W., Abbaspour, K.C., White, M.J., Srinivasan, R., Santhi, C., Harmel, R.D., van Griensven, A., Van Liew, M.W. & Kannan, M.K.J. (2012). SWAT: Model use, calibration, and validation. Transactions of ASABE, 55(4),1491-1508.

Janssen, J.M. (2020). Estimating new reservoir locations with the use of a hydrological model for small holder cotton farmers in Maharashtra , India. Msc. thesis, The Delft University of Technology, Netherlands, 1-133.

Jassogne, L., Läderach, P. & van Asten, P. (2013). Impact of Climate Change on Coffee in Uganda. Lessons from a Case Study in Rwenzori Mountains. Oxfarm Research Reports (April),Oxfam GB, 1-16.

Jia, C., Sun, B., Yu, X. & Yang, X. (2020). Analysis of runoff and sediment losses from a sloped roadbed under variable rainfall intensities and vegetation conditions.Sustainability (Switzerland), 12(5),1-11.

Junqueira, J.P., Ponzo, A.P.S. & Oliveira, A.S. (2020). Viability of a terrace covered with porous concrete paving blocks for coffee bean drying. Comissão editorial, 12(4), 98.

Kagwanja, P. (2007). Calming the Waters: The East African Community and Conflict over the Nile Resources. Journal of Eastern African Studies, 1(3), 321-337.

Kaviya, B. (2013). Runoff estimation using SWAT Model in Brahmani-Baitarani River Basin.

International Journal of Biotech Trends and Technology (IJBTT), 3(2), 1-16.

Khudhair, M.A., Sayl, K.N. & Darama, Y. (2020). Locating Site Selection for Rainwater Harvesting Structure using Remote Sensing and GIS. IOP Conference Series: Materials Science and Engineering, 881(012170), 1-10.

Kiggundu, N., Wanyama, J., Mfitumukiza, D., Twinomuhangi, R., Barasa, B., Katimbo, A. & Kyazze, F.B. (2018). Rainwater harvesting knowledge and practice for agricultural production in a changing climate: A review from Uganda's perspective. Agricultural Engineering International: CIGR Journal, 20(2), 19-36.

Kimera, F., Sewilam, H. & Imam, E. (2018). Economic Benefits of Supplemental Irrigation in Uganda. Agricultural Sciences, 9(11), 1401-1418.

Kisakye, V., Akurut, M. & Bruggen, B. (2018). Effect of climate change on reliability of rainwater harvesting systems for Kabarole District, Uganda. Water (Switzerland), 10(71), 1-35.

Kisekka, J., Kinaalwa, N., Busingye, E. & Onneweer, M. (2018). Fostering the use of rainwater for food security in Rwenzori Region, Uganda. Rainwater-Smart Agriculture in Arid and Semi-Arid Areas, 8(17), 1-20.

Koskei, C.E. (2016). Rainfall variability and use of Rainwater harvesting as an adaptation strategy for climate change in Baringo county. Ph.D thesis, Kabarak University, Kenya, 1-243.

Kouchi, D.H., Esmaili, K., Faridhosseini, A., Sanaeinejad, S.H., Khalili, D. & Abbaspour, K.C. (2017). Sensitivity of calibrated parameters and water resource estimates on different objective functions and optimisation algorithms.Water (Switzerland), 9(384), 1-16.

Laouisset, M.B. & Dellal, A. (2016). Estimation of barley crop water requirements using cropwat software in Ksar-Chellala Region, Algeria. Agris On-line Papers in Economics and Informatics, 8(3), 91-102.

Li, K., Wang, Y.Q., Xu, J.J., Hong, X.F. & Feng, Y. (2020). Runoff simulation of Tangnaihai hydrological station in source area of Yellow River based on SWAT model. IOP Conference Series: Earth and Environmental Science, 612(012047), 1-9.

MAAIF. (2017). National Irrigation Policy, Ministry of Agriculture, Animal Industry and Fisheries and Ministry of Water and Environment, Issue (November), Republic of Uganda, 1-35.

MAAIF. (2020). Technical Guideline for Small Gravity Irrigation Schemes in Uganda, Ministry of Agriculture, Animal Industry and Fisheries, Issue (June), Republic of Uganda, 1-73.

Maher, S., Lisa, B., Motasem, A., Cecilia, B., Laura, G., Otto, H., Francesco, S. & Frank van, S. (2016). Status, performance and scope assessment of water harvesting in Uganda, Burkina Faso and Morocco. Strengthening agricultural water efficiency and productivity on African and global level, FAO, Rome, 1-59.

Mahmoud, S.H., Mohammad, F.S. & Alazba, A.A. (2015). Delineation of potential sites for rainwater harvesting structures using a geographic information system-based decision support system. Hydrology Research, 46(4), 591-606.

Maidment, D.R., Rassmusson, E., Dickinson, R., Smith, J., Shuttleworth, W. & Rawls, W.J. (1993).

Handbook of Hydrology,University of Texas at Austin, AIT Library McGraw-Hill -New York, 1-1143.

Manandhar, R., Odehi, I.O.A. & Ancevt, T. (2009). Improving the accuracy of land use and land cover classification of landsat data using post-classification enhancement. Journal of Remote Sensing, 1(3), 330-344.

Manaouch, M., Sadiki, M. & Fenjiro, I. (2021). Integrating WaTEM / SEDEM model and GIS-based FAHP Method for Identifying Ecological Rainwater Harvesting Sites in Ziz upper watershed , SE Morocco. Research Square, 1-21.

Matomela, N., Li, T. & Ikhumhen, H.O. (2020). Siting of Rainwater Harvesting Potential Sites in Arid or Semi-arid Watersheds Using GIS-based Techniques. Environmental Processes, 7(2), 631-652.

MCDonnel, T. (2017). A Drying Climate threatens Africa's Coffee, But Hope Remains, National Geographic Report, August Issue, Uganda,1-20.

Meena, S.R., Ghorbanzadeh, O., van Westen, C.J., Nachappa, T.G., Blaschke, T., Singh, R.P. & Sarkar, R. (2021). Rapid mapping of landslides in the Western Ghats (India) triggered by 2018 extreme monsoon rainfall using a deep learning approach. Journal of Landslides, 18(6), 1937-1950.

Miito, G.J. & Banadda, N. (2017). A short review on the potential of coffee husk gasification for sustainable energy in Uganda. F1000Research, 6(1809), 1-12.

Mishra, A. (2014). Soil & Water Conservation Engineering Lecture notes by Professor. Ashok Mishra, Department of Agricultural and Food Engineering. Lesson 28, Indian Institute of Technology Kharagpur, 1-12.

Mohan, A., Singh, A.K., Kumar, B. & Dwivedi, R. (2021). Review on remote sensing methods for landslide detection using machine and deep learning. Transactions on Emerging Telecommunications Technologies, 32(4), 1-23.

Moriasi, D.N., Arnold, J.G., Van Liew, M.W., Bingner, R.L., Harmel, R.D. & Veith, T.L. (2007). Model Evaluation Guidelines for Systematic Quantification of Accuracy in Watershed Simulations. 50(3), 855–900.

Mosase, E., Kayombo, B., Tsheko, R. & Tapela, M. (2017). Assessment of the Suitability of Rain Water Harvesting Areas Using Multi-Criteria Analysis and Fuzzy Logic. Advances in Research, 10(4), 1-22.

Moseki, O., Murray-Hudson, M. & Kashe, K. (2019). Crop water and irrigation requirements of Jatropha curcas L. in semi-arid conditions of Botswana: applying the CROPWAT model. Agricultural Water Management, 225(105754), 1-7.

Mourad, K. & Berndtsson, R. (2011). Potential water saving from Rainwater harvesting in Syria. Vatten, 67(1), 113-117.

Mugerwa, N. (2007). Rainwater harvesting and rural livelihood improvement in banana growing areas of Uganda, MSc.thesis, Linköping University, Sweden, 1-60.

Mukasa, J., Olaka, L. & Said, M.Y. (2020). Drought and households' adaptive capacity to water scarcity in Kasali, Uganda. Journal of Water and Climate Change, 11(S1), 217-232.

Mulualem, A. & Yegizaw, E.S. (2018). Potential rainwater harvesting suitable land selection and management by using GIS with MCDA in Ebenat District, Northwestern Ethiopia. Journal of Degraded and Mining Lands Management, 8(1), 2537-2549.

Munyao, J.N. (2010). Use of Satellite products to assess rainwater harvesting potential in remote areas of Africa. Msc.thesis, International Institute of Geo-information Science and Earth Observation, Netherlands,1-80.

Munyuli, M.B.T. (2012). Micro, local, landscape and regional drivers of bee biodiversity and pollination services delivery to coffee (Coffea canephora) in Uganda. International Journal of Biodiversity Science, Ecosystem Services and Management, 8(3), 190-203.

Msuya, A.M. (2013). Impact of Climate Variability on Coffee Production and Farmers' Copying and Adaptation Strategies in Highlands of Kigoma District, Msc.thesis, Sokoine University of Agriculture, Morogoro, Tanzania, 1-72.

MWE. (2016). Handbook on Rainwater Harvesting and Storage options. Ministry of Water and Environment, Republic of Uganda, 1-79.

MWE. (2019a). Kabuyanda Irrigation Scheme- Environmental and Social Impact Assessment Report, Irrigation for Climate Resilience Project - P163836, September Report, Ministry of Water and Environment, Republic of Uganda, 1-556.

MWE. (2019b). Water and Environment Sector Development Plan 2015/16-2019/20, Ministry of Water and Environment, Republic of Uganda, 1-145.

MWE. (2020a). Water and Environment Sector Performance Report. Ministry of Water and Environment, Issue (Sepetember), Government of Uganda, 1-342.

MWE. (2020b). Water and Environment Sector Performance Report. Ministry of Water and Environment, Issue (Sepetember), Republic of Uganda, 1-374.

MWE. (2022). Directorate of Water Development, Ministry of Water and Environment. Uganda Water Supply Atlas, Isingiro District, Republic of Uganda, 1-6.

MWE & MAAIF. (2020). Irrigation for Climate Resilience Project Abstract. Ministry of Water and Environment and Ministry of Agriculture, Animal Industries and Fisheries, Issue (Sepetember), Republic of Uganda, 1-2.

Naghibi, S.A., Ahmadi, K. & Daneshi, A. (2017). Application of Support Vector Machine, Random Forest, and Genetic Algorithm Optimised Random Forest Models in Groundwater Potential Mapping. Water Resources Management, 31(9), 2761-2775.

Nakawuka, P., Langan, S., Schmitter, P. & Barron, J. (2018). A review of trends, constraints and opportunities of smallholder irrigation in East Africa. Global Food Security, 17(11), 196-212.

Nalunga, A. (2021). Essays on the coffee supply chain in Uganda. Ph.D. thesis, Kansas state Uniersity, Manhattan-Kansas,1-160.

Narmilan, A. & Sugirtharan, M. (2021). Application of FAO-CROPWAT Modelling on Estimation

of Irrigation Scheduling for Paddy Cultivation in Batticaloa District, Sri Lanka. Agricultural Reviews, 42(1), 73-79.

Nilawar, A.P. & Waikar, M.L. (2018). Use of SWAT to determine the effects of climate and land use changes on streamflow and sediment concentration in the Purna river basin, India. Environmental Earth Sciences, 77(783), 1-13.

Nyasimi, M., Radeny, M., Mungai, C. & Kamini, C. (2016). Uganda's National Adaptation Programme of Action: Implementation, Challenges and Emerging Lessons. CGIAR Research Program on Climate, Agriculture and Food Security (CCAFS), 1-36.

Nyirenda, F., Mhizha, A., Gumindoga, W. & Shumba, A. (2021). A GIS-based approach for identifying suitable sites for rainwater harvesting technologies in Kasungu District, Malawi. Water SA, 47(3), 347-355.

O'Hanlon, F., Lantagne, D.S., Morgan, D. & William, N. (2020). Maintenance practices and water quality from rainwater harvesting in South-Western Uganda. Journal of Water Sanitation and Hygiene for Development, 10(3), 549-557.

Onyutha, C., Turyahabwe, C. & Kaweesa, P. (2021). Impacts of climate variability and changing land use/land cover on River Mpanga flows in Uganda, East Africa. Environmental Challenges, 5(100273), 1-14.

Opiña, P.V. & Corpuz, R.R. (2021). Suitability Mapping of Small Farm Reservoirs Using K-Nearest Neighbors And Random Forest Algorithms. International Journal of Scientific and Technology Research, 10(3), 78-80.

Oweis, T.Y. & Hachum, A.Y. (2003). Improving Water Productivity in the Dry Areas of West Asia and North Africa. International Center for Agricultural Research in the Dry Areas, Water Management and Irrigation Engineering, University of Mosul, Iraq, 179-198.

Oweis, T.Y., Prinz, D. & Hachum, A.Y. (2012). Rainwater harvesting for agriculture in the dry areas. International center for Agricultural Research in Dry Areas (ICARDA), Syria, 1-276.

Plourde, L. & Congalton, R.G. (2003). Sampling method and sample placement: How do they affect the accuracy of remotely sensed maps?. Photogrammetric Engineering and Remote Sensing, 69(3), 289-297.

Prakash, N., Manconi, A. & Loew, S. (2020). Mapping landslides on EO data: Performance of deep learning models vs Traditional machine learning models. Journal of remote sensing, 12(3), 346.

Prijono, S. & Sidauruk, I.P. (2020). Analysis of soil moisture storage by using various rainwater harvesting methods at people's coffee plantation. Soil Science Department, Faculty of Agriculture, University of Brawijaya, East Java, Indonesia, 26(4),1520-1526.

Rahmati, O., Pourghasemi, H.R. & Melesse, A.M. (2016). Application of GIS-based data driven random forest and maximum entropy models for groundwater potential mapping: A case study at Mehran Region, Iran. Catena, 137, 360–372.

Rana, V.K. & Maruthi, T.S.V. (2020). GIS-based multi criteria decision making method to identify potential runoff storage zones within watershed. Annals of GIS, 26(2), 149-168.

Rasul, G.F.I., Rasul, A., Hamid, A.A., Ali, Z.F. & Dewana, A.A. (2019). Suitable Site Selection for Rainwater Harvesting and Storage Case Study Using Dohuk Governorate. Journal of Water, 11(864), 1-17.

Refsgaard, J.C. (1997). Parameterisation, calibration and validation of distributed hydrological models. Journal of Hydrology, 198(1), 69-97.

Rockström, J. & Falkenmark, M. (2015). Increase water harvesting in Africa. Meeting global food needs requires strategies for storing rainwater and retaining soil moisture to bridge dry spells. Macmillan Publishers Limited, 519(1), 283-285.

RoU. (2020a). Barrier Analysis and Enabling Framework Report-1. Technology Needs Assessment For Climate Change Adaptation in Agriculture, Water and Forestry Sectors of Uganda, Republic of Uganda, 1-185.

RoU. (2020b). Barrier Analysis and Enabling Framework Report-2. Technology Needs Assessment For Climate Change Adaptation in Agriculture, Water and Forestry Sectors of Uganda, Republic of Uganda, 1-164.

RoU. (2020c). Isingiro District Local Government Multi-Hazzard Contigency Plan, Republic of Uganda, 1-62.

Rouholahnejad, E., Abbaspour, K.C., Vejdani, M., Srinivasan, R., Schulin, R. & Lehmann, A. (2012). A parallelisation framework for calibration of hydrological models. Environmental Modelling and Software, 31(1), 28-36.

Ruan, H., Zou, S., Yang, D., Wang, Y., Yin, Z., Lu, Z., Li, F. & Xu, B. (2017). Runoff simulation by SWAT model using high-resolution gridded precipitation in the upper Heihe River Basin, Northeastern Tibetan Plateau. Water (Switzerland), 9(866), 1-22.

Rwanga, S.S. & Ndambuki, J.M. (2017). Accuracy Assessment of Land Use/Land Cover Classification Using Remote Sensing and GIS. International Journal of Geosciences, 8(4), 611-622.

Satheeshkumar, S., Venkateswaran, S. & Kannan, R. (2017). Rainfall–runoff estimation using SCS–CN and GIS approach in the Pappiredipatti watershed of the Vaniyar sub basin, South India. Modeling Earth Systems and Environment, 3(24), 1-8.

Sayl, K.N., Mohammed, A.S. & Ahmed, A.D. (2020). GIS-based approach for rainwater harvesting site selection. IOP Conference Series: Materials Science and Engineering, 737 (012246), 1-11.

Shanbor, K. & Manoj, J. (2017). Rainfall-Runoff Modeling of a River Basin using SWAT Model. International Journal of Engineering Research and Technology, 6(12), 293-302.

Sitterson, J., Knightes, C., Parmar, R., Wolfe, K., Muche, M. & Avant, B. (2017). An Overview of Rainfall-Runoff Model types. The United States Environmental Protection Agency report. Office of Research and Development National Exposure Research Laboratory Athens, Georgia, 1-30.

Smith, M. (1992). CROPWAT: A computer program for irrigation planning and management. Food and Agricultural Organisation Irrigation and Drainage Paper 46, Rome, Italy, 1-128.

Sridharan, V., Ramos, E. P., Zepeda, E., Boehlert, B., Shivakumar, A., Taliotis, C. & Howells, M. (2019). The impact of climate change on crop production in Uganda-An integrated systems assessment with water and energy implications. Water (20734441), 11(1805), 1-25.

Ssenyimba, S., Kiggundu, N. & Banadda, N. (2020). Designing a solar and wind hybrid system for small scale irrigation: A case study for Kalangala district in Uganda. Energy, Sustainability and Society, 10(6), 1-18.

Staddon, C., Rogers, J., Warriner, C., Ward, S. & Powell, W. (2018). Why doesn't every family practice rainwater harvesting? Factors that affect the decision to adopt rainwater harvesting as a household water security strategy in central Uganda. Water International, 43(8), 1114–1135.

Stancalie, G., Marica, A. & Toulios, L. (2010). Using earth observation data and CROPWAT model to estimate the crop evapotranspiration. Physics and Chemistry of the Earth, 35(1), 25-30.

Stanley, M.H., Mudahemuka, W., Siraje, K.P. & Asiimwe, S. (2020). Contribution of Run-off Water Harvesting to Food Production in Kyannamukaaka Sub County, Uganda. Journal of Research Innovationand Implications in Education, 4(3), 9-18.

Strahler, A.H., Boschetti, L., Foody, G.M., Friedl, M.A., Hansen, M.C., Herold, M., Mayaux, P., Morisette, J.T., Stehman, S.V. & Woodcock, C.E. (2006). Global Land Cover Validation: Recommendations for Evaluation and Accuracy Assessment of Global Land Cover Maps.Luxemburg: Office for Official Publications of the European Communities, GOFC-GOLD Report No. 25, 1-60.

Tan, M.L., Gassman, P.W., Yang, X. & Haywood, J. (2020). A review of SWAT applications, performance and future needs for simulation of hydro-climatic extremes. Advances in Water Resources, 1-55.

Taunk, K., De, S., Verma, S. & Swetapadma, A. (2019). A brief review of Machine Learning Classification with K-Nearest Neighbours. Research Gate, Conference paper, 1-11.

Thao, N.T.T., Khoi, D.N., Xuan, T.T. & Tychon, B. (2019). Assessment of Livelihood Vulnerability to Drought: A Case Study in Dak Nong Province, Vietnam. International Journal of Disaster Risk Science, 10(4), 604-615.

Tobergte, D.R. & Curtis, S. (2013). Growing Lemons in Australia - A Production Manual. Journal of Chemical Information and Modeling, 53(9), 1689–1699.

Toosi, A.S., Tousi, E.G., Ghassemi, S.A., Cheshomi, A. & Alaghmand, S. (2020). A multi-criteria decision analysis approach towards efficient rainwater harvesting. Journal of Hydrology, 582(124501), 1-14.

Tsendbazar, N., Li, L., Koopman, M., Carter, S., Herold, M., Georgieva, I. & Lesiv, M. (2021). European Space Agency World Cover 2020 Map Version 100, Product Validation Report, Zenodo,1-38.

UBOS. (2021). System of Environmental Economic Accounting, Uganda Water Accounts Report, Uganda, 1-40.

UCDA. (2006). Uganda Coffee Development Authority, Annual Report, October 01, 2005 -

September 30, 2006, Volume 15. Ministry of Agriculture, Animal Industries and Fisheries, Uganda, 1-82.

UCDA. (2013). Uganda Coffee Development Authority, Annual Report, October 01, 2011 – September 30, 2012, Volume 21. Ministry of Agriculture, Animal Industries and Fisheries, Uganda, 1-104.

UCDA. (2017). Uganda Coffee Development Authority, Annual Report, July 01, 2015 – June 30, 2016, Volume 25. Ministry of Agriculture, Animal Industries and Fisheries, Uganda, 1-91.

UCDA. (2019a). A Sustainable Coffee Industry with High Stakeholder Value for Social Economic Transformation, Arabica Coffee Handbook, First edition, Uganda Coffee Development Authority, Uganda, 1-138.

UCDA. (2019b). A Sustainable Coffee Industry with High Stakeholder Value for Social Economic Transformation. Robusta Coffee Handbook, First Edition, Uganda Coffee Development Authority, Uganda, 1-148.

UCDA. (2022). A sustainable coffee industry with high stakeholder value for social economic transformation, Directorate of Strategy and Business Development, Issue (January), Uganda Coffee Development Authority,Uganda, 1-10.

URWA. (2013). A Construction Documentation for the Promotion of 3R (Recharge, Retention and Re-Use). Uganda Rainwater Association, Uganda, 1-32.

Velasco-Muñoz, J.F., Aznar-Sánchez, J.A., Batlles-delaFuente, A. & Fidelibus, M. D. (2019). Rainwater harvesting for agricultural irrigation: An analysis of global research. Water (Switzerland), 11(7), 1-18.

Verter, N., Bamwesigye, D. & Darkwah, S.A. (2015). Analysis of Coffee Production and Exports in Uganda. International Conference on Applied Business Research, 1(613), 1-9.

Wang, N., Jassogne, L., van Asten, P.J.A., Mukasa, D., Wanyama, I., Kagezi, G. & Giller, K.E. (2015). Evaluating coffee yield gaps and important biotic, abiotic, and management factors limiting coffee production in Uganda. European Journal of Agronomy, 63(1), 1-11.

Wangui, K.J. (2012). Effects of Climate Variability on Large Scale Coffee Production in Kigutha Coffee Estate in Kiambu, Kenya, Msc.thesis, Kenyatta University, Kenya, 1-99.

Wanyama, J., Ssegane, H., Kisekka, I., Komakech, A.J., Banadda, N., Zziwa, A., Ebong, T.O., Mutumba, C., Kiggundu, N. & Kayizi, R.K. (2017). Irrigation Development in Uganda : Constraints , Lessons Learned , and Future Perspectives. 143(1).

Worku, T., Khare, D. & Tripathi, S.K. (2017). Modeling runoff–sediment response to land use/land cover changes using integrated GIS and SWAT model in the Beressa watershed. Environmental Earth Sciences, 76(550), 1-15.

Yamaç, S.S. (2021). Artificial intelligence methods reliably predict crop evapotranspiration with different combinations of meteorological data for sugar beet in a semiarid area. Agricultural Water Management, 254(9), 1-13.

Ziadat, F., Bruggeman, A., Oweis, T., Haddad, N., Mazahreh, S., Sartawi, W. & Syuof, M. (2012).

A Participatory GIS Approach for Assessing Land Suitability for Rainwater Harvesting in an Arid Rangeland Environment. Arid Land Research and Management, 26(4), 297-311.

Zou, S., Ruan, H., Lu, Z., Yang, D., Xiong, Z. & Yin, Z. (2016). Runoff simulation in the upper reaches of Heihe river basin based on the RIEMS-SWAT model. Water (Switzerland), 8(455), 1-16.

Zziwa, A., Kyazze, F.B., Kiggundu, N. & Namubiru, E. (2018). Rainwater Harvesting practices for improving climate adaptation for farmers in Uganda. The Technical Centre for Agricultural and Rural Cooperation ACP-EU (CTA), Wageningen, Netherlands, 1-48.